AgEcon SEARCH
RESEARCH IN AGRICULTURAL & APPLIED ECONOMICS

*The World's Largest Open Access Agricultural & Applied Economics Digital Library*

**This document is discoverable and free to researchers across the globe due to the work of AgEcon Search.**

**Help ensure our sustainability.**

Give to AgEcon Search

AgEcon Search
http://ageconsearch.umn.edu
aesearch@umn.edu

*Papers downloaded from **AgEcon Search** may be used for non-commercial purposes and personal study only. No other use, including posting to another Internet site, is permitted without permission from the copyright owner (not AgEcon Search), or as allowed under the provisions of Fair Use, U.S. Copyright Act, Title 17 U.S.C.*

*No endorsement of AgEcon Search or its fundraising activities by the author(s) of the following work or their employer(s) is intended or implied.*

Copyright 2024 by Jingfang Zhang, Emir Malikov, Ruiqing Miao, Prasenjit Ghosh. All rights reserved. Readers may make verbatim copies of this document for non-commercial purposes by any means, provided this copyright notice appears on all such copies.

# Geography of Climate Change Adaptation in U.S. Agriculture: Evidence from Spatially Varying Long-Differences Approach*

JINGFANG ZHANG[1] EMIR MALIKOV[2] RUIQING MIAO[3] PRASENJIT GHOSH[4]

[1]Alcorn State University
[2]University of Nevada, Las Vegas
[3]Auburn University
[4]University of Southern Indiana

October 31, 2023

**Abstract**

Geography is a salient feature in agricultural adaptation to a warming climate. Facing heterogeneous natural-resource and climatic endowments, farmers in different locations choose adaptive strategies that are best suited to their environments, resulting in inhomogeneous adaptation across space. We provide novel evidence of this *explicitly spatial* heterogeneity in heat sensitivity of U.S. crop yields and their adaptation thereto. We generalize a popular long-differences approach by explicitly incorporating geographic information of crop-producing counties in a semiparametric fashion, using local kernel averaging. This lets us control for spatially clustered local heterogeneity that may be non-neutral in that it mediates climate effects on agriculture. Obtained measurements of historical adaptation are also more granular and account for local contexts, as do projected yield changes due to climate change. We find that corn and soybean adaptation to overheat mainly occurred in the Northern Great Plains and Upper Midwest; and for cotton, in the Mississippi Delta. There is a geographic bifurcation in expected climate change effects by the mid-century, with some regions projected to experience large yield declines and others to benefit from significant yield gains. Considering the net offset potential of this bifurcation, our average yield impact projections are generally smaller compared to traditional approaches.

**Keywords**: Climate Change, Crop Yield, Heterogeneity, Panel Data, Spatially Varying Coefficient

## 1 Introduction

The changing climate has been posing an increasing threat to sustainable agricultural production as extreme heat and drought episodes become increasingly frequent (Semenov and Shewry, 2011; Rahmstorf and Coumou, 2011; Field et al., 2012; Gourdji et al., 2013; Trnka et al., 2014). Understanding adaptation to a warming climate is critical to measuring the damages of climate change for agriculture. In the spirit of a typical analysis of average treatment effects on the treated, prior studies that examine whether—and to what

* *Correspondence to*: emir.malikov@unlv.edu (Malikov).

extent—the adaptation to climate change occurs in agriculture almost exclusively focus on identification of the *average* adaptation (e.g., Burke and Emerick, 2016; Blanc and Schlenker, 2017; Malikov et al., 2020; Chen and Gong, 2021; Mérel and Gammans, 2021; Yu et al., 2021; Cui and Xie, 2022; Moscona and Sastry, 2022). While interesting in its own right, by construction, such a global estimand sheds little light on *local* adaptation experiences of farmers which, in all likelihood, exhibit substantial geographical heterogeneity. Crop producers in different locations deal with heterogeneous natural-resource and climatic endowments, likely employing different farming practices. Such persistent geographic differences may also prompt farmers to choose various adaptation strategies that are more optimally suited to the specific environment they face, leading to inhomogeneous adaptation outcomes across space. Understanding this (naturally occurring) spatial heterogeneity is first-order for producing more granular measurements of historical adaptation and, by extension, more accurate projections of future agricultural yield losses associated with climate change, particularly in large and climatically diverse countries.

In this paper, we provide novel evidence of *explicitly spatial* heterogeneity in heat sensitivity of U.S. agriculture and adaptation thereof to a warming climate. When modeling the long-run relationship between agriculture and climate, we allow the time-variant responsiveness of mean crop yields to climate (particularly, to excessively high temperatures) to vary across geographic locations, thus capturing local heterogeneity in farmers' adaptation capabilities. To measure this cross-location variability, we employ a semiparametric varying-coefficient panel-data model in the vein of Hastie and Tibshirani (1993), Cai et al. (2000) and Li et al. (2002), capable of accommodating spatially inhomogeneous county-specific relationships between climate and agriculture that can systematically vary across geography and over time.

Concretely, we let temporally varying coefficients in the mean projection of crop yields on climate variables in a county be nonparametric functions of the county's geographic location. This enables us to control for local heterogeneity that needs not be additively separable (i.e., climate-neutral), as typically restricted by means of intercept-shifting county fixed effects. Our treatment of the cross-county spatial heterogeneity is more flexible in that we let it be nonneutral so that it can also mediate local climate effects on agricultural yields by, in effect, also shifting slopes. As such, our analytical strategy is more general than go-to (fully parametric) methodologies for modeling the climate-agriculture relationship—both the "fixed-effects" (e.g., Schlenker and Roberts, 2009; Chen et al., 2016; Miao et al., 2016; Cui, 2020) and "long differences" approaches (e.g., Burke and Emerick, 2016; Yu et al., 2021)—because not only do we allow the estimated relationship to vary between individual counties but, most of all, we do so in a manner that explicitly recognizes the contiguous *geography* of climate change.

For identification we only require that marginal effects of climate vary across space smoothly, beyond which we continue to maintain the assumption of strict exogeneity of within-county climate variation customarily made in panel-data studies. Because the geographic smoothing variables are time-invariant for counties and thus unaffected by differencing or within transformation, our kernel estimation is *not* complicated by the presence of additive unit fixed effects. This is notable because, otherwise, transforming fixed effects out of semi/nonparametric panel-data regressions may add to bias, worsen convergence rates, involve multi-step implementation and/or cumbersome techniques such as back-fitting or marginal integration (e.g., see Sun et al., 2009; Su and Ullah, 2011; Rodríguez-Póo and Soberón, 2015; Malikov et al., 2016).

Spatiotemporally varying coefficients in our model are set to parsimoniously capture the myriad unobserved and observed factors pertaining to each county's geographic location that may influence the sensitivity of agricultural yields to climate variation, including agricultural practices, the quality of soil, local institutions and regulations, as well as many persistent features of the local climatic system which shape farming.[1] Technological opportunities and management strategies vary across space as well. Farmers dealing with particular land quality and other geotopographic endowments correspondingly adopt different field management practices, e.g., the application of fertilizers, irrigation, use of improved seeds, employment of rotation and tillage types. Farmers' perception of climate change across different locations also need not be the same (see Burke and Emerick, 2016). For instance, a local extreme heat event in early periods might signify a warming climate from local farmers' point of view and prompt them to adopt adaptation and mitigation strategies more proactively than typically. Spatially heterogeneous institutional and regulatory environments also prompt farmer's differential choices of adaptation strategies across regions (see World Bank, 2008; Bogdanski, 2012; Scherr et al., 2012).

In light of some concerns in the literature that, to identify the climate sensitivity of agriculture, standard fixed-effects estimators rely on the annual weather variation instead of the long-run climate change (see Blanc and Schlenker, 2017; Chen and Gong, 2021), in our analysis we adopt Burke and Emerick's (2016) alternative "long differences" approach as a modeling paradigm to study climate change adaptation. The idea is simple: estimating the climate-agriculture relationship using temporal differences in the longer-run local averages, we can identify the effect of "climate" on agriculture. However, we generalize this approach

[1] While some of these factors—notably, regulations and farming practices—may be endogenous with respect to agricultural productivity, the county's geographic location which we effectively use as their proxy is however immune to these concerns given its plausibly strict exogeneity.

in a critical aspect. Namely, both the original Burke and Emerick's (2016) long-differences methodology and its recent time-varying extension by Yu et al. (2021) focus on measuring *average* (over cross-sectional units and, by implication, space) causal effects of climate on agricultural productivity. To identify these effects, they implicitly assume that confounding cross-sectional heterogeneity is strictly additive (shifts the intercept only) and thus can be fully controlled for via additively separable fixed effects. Using both data-driven methods and formal inference, we find that the latter is not corroborated empirically. Our analysis reveals strong evidence that local heterogeneity—proxied by geographic location—also plays a significant role in mediating the yield-climate relationship, influencing marginal effects of climate. Given the naturally occurring correlation between the county location and local climate variation, ignoring such non-additive spatial heterogeneity can result in omitted time-varying confounders, thus hindering identification of even the average climate effect via standard fixed-coefficient estimators. With the data rejecting spatial invariance of slopes, we therefore build an approach that explicitly accommodates non-neutral spatiotemporal heterogeneity in the climate effects on agriculture by allowing regression parameters to change with location and over time. As such, our paper contributes to the climate literature on a methodological front by providing a framework which generalizes the popular long-differences approach in a practically important aspect.

Our analysis is based on county-level crop yields for corn, soybeans, and cotton and climate data in the rain-fed region of the United States during the 1958–2019 period. With data-driven cross-validation and formal specification tests rejecting a go-to spatially invariant specification across an array of popular models for measuring marginal effects of climate, we find that sensitivity and adaptation of crop yields to a warming climate vary significantly across space. This variation is not haphazard either. For corn yields, 54% of counties are estimated to have experienced statistically significant decreases in overheat sensitivity (termed "adaptation"), 12% to have experienced statistically significant *increases* (termed "maladaptation"), and 34% to have had *no* statistically significant changes (termed "no adaptation"). For soybeans, the three corresponding numbers are 75%, 2%, and 23%; for cotton, they are 23%, 77%, and 0%. Geographically, corn and soybean adaptation to overheat mainly occurred in the Northern Great Plains and Upper Midwest; for cotton, it occurred in the Mississippi Delta. On acreage-weighted average, our model estimates that yield sensitivity of corn, soybeans, and cotton to overheat respectively declined by 73%, 49%, and 51% over 1958–2019, although for cotton this decrease was statistically insignificant. Of note, spatially invariant specifications tend to produce larger estimates of declines in overheat sensitivity. This underscores potential perils of abstracting away from naturally occurring non-neutral spatial heterogeneity when measuring marginal effects of climate on agriculture, which may result in overestimated evidence of (mal)adaptation.

Accounting for significant spatial heterogeneity when projecting expected damages of a warming climate between the end of our sample period (2015–2019) and the mid-century (2048–2052), we find a clear geographic bifurcation in future climate change effects on yields. For corn production, some regions in the lower Midwest (Nebraska, Kansas, southern Iowa, northern Missouri and parts of South Dakota) and South (Tennessee, Georgia, South Carolina, northern Alabama) are projected to experience large declines in yield by 2048–2052. Whereas, parts of the Corn Belt including some areas in Indiana, Ohio, Illinois, and part of North Dakota are expected to benefit from significant yield gains due to a warming climate. Owing to its spatial flexibility, which enables us to capture this bifurcation, our methodology generally produces *smaller* yield loss/gain projections, compared to traditional spatially invariant alternatives. As such, our yield loss projection are much smaller relative to earlier studies (e.g., Burke and Emerick, 2016; Yu et al., 2021). On acreage-weighted average for the whole rain-fed U.S., depending on a climate change scenario, by 2048–2052 our model predicts 7–13% yield losses for corn, 12–48% yield losses for soybeans, and 5–24% yield gains for cotton relative to their 2015–2019 levels, although these average projections for corn and cotton are statistically insignificant. This result is intuitive given the spatial bifurcation in future climate change effects on crop productivity, with the offset potential in the net average effect. Across regions, however, the effects are not net-zero.

To summarize, the contribution of our paper is as follows. We expand the frontier of climate economics literature by studying explicitly spatial heterogeneity in heat sensitivity of the U.S. agriculture and its adaptation to a warming climate. Our analysis relaxes the empirically uncorroborated space-invariance assumption which, if violated, may jeopardize identification of (average) marginal effects of climate. To this end, we generalize a popular long-differences approach to accommodate non-neutral local heterogeneity. Our modeling framework is more flexible in that it parsimoniously accounts for many (un)observed local factors that may mediate climate effects on agricultural production. Our paper shows that, without considering spatial variation in adaptation, standard approaches tend to overestimate yield damages of climate change.

Although understudied, our focus on spatial heterogeneity in the climate sensitivity of agricultural production is not without precedent. In this regard, our paper complements the earlier work by Butler and Huybers (2013) and Keane and Neal (2020) who investigate non-neutral cross-county heterogeneity in the effects of weather/climate on mean crop yields.[2] Unlike Butler and Huybers' (2013) approach, ours mea-

[2] Some studies investigate time-varying sensitivity of crop yields to weather variation (e.g., see Schlenker and Roberts, 2009; Roberts and Schlenker, 2011, 2012; Lobell et al., 2014), but spatial heterogeneity is not their focus.

sures the adaptation to a warming climate in a flexible way without needing to rely on ad-hoc time-invariant parameterizations of heat sensitivity of yields: instead, we let the latter change over time arbitrarily. On the other hand, to identify cross-county and cross-time heterogeneity in marginal effects of climate, in contrast to Keane and Neal (2020), we do not assume additive time and unit fixed effects in slopes, meaning that spatial heterogeneity in climate sensitivity of yields in our analysis need not be time-invariant. The critical implication is that our methodology, unlike Keane and Neal's (2020), facilitates the analysis of cross-location differences in the *adaptation* to a warming climate *over time*.[3] Also, for consistency our approach requires large-$n$ asymptotics, whereas the above alternatives can deliver consistent estimation only when $T$ (Butler and Huybers, 2013) or even both $T$ and $n$ (Keane and Neal, 2020) diverge. While theoretical, these nuances can have important practical implications in finite samples, given that most yield-climate analyses utilize large-$n$-small-$T$ panels.

More importantly, although these prior studies also examine the variation in climate-agriculture relationship across counties and even interpret such heterogeneity as "spatial," neither one explicitly incorporates *spatial* information into their modeling. As such, conceptually, a more appropriate characterization of the heterogeneity that they document between counties is perhaps "cross-sectional." In contrast, our approach to measuring cross-county heterogeneity in climate change effects and adaptation thereto is implemented by explicitly recognizing the geographic location of each county. This is a non-trivial distinction because both climate and soil quality are inherently linked to the county's location; both are spatially contiguous and not assigned arbitrarily. By letting the climate effects on yields expressly depend on location via smooth slope functions and estimating them nonparametrically by locally averaging over spatially proximate counties, we directly leverage this contiguity and clustering across space in the data. To this end, the cross-county heterogeneity in climate change adaptation that our model is able to identify is unambiguously spatial. Incidentally, Park et al. (2023) have also studied geographic variation in climate effects on agricultural yields, whereby they build a Bayesian spatially varying functional model to forecast county-level corn yield in five Midwest states. Our paper is distinct from theirs in its methodological approach (including controlling for unobservable county-level confounders), significantly larger empirical scope and, most importantly, our main focus on spatially inhomogeneous *adaptation* to climate change over time.

The rest of the paper is organized as follows. Section 2 introduces methodology and the corresponding estimation strategy. Section 3 documents data, followed by the discussion of empirical results about spatial

[3] In Keane and Neal (2020), temporal changes in county-specific slopes do not vary across units by assumption, a priori imposing that all counties adapt to climate change over time exactly the same. As already noted, we find that the data do not support this.

heterogeneity of climate change effects on agriculture and the adaptation thereto by farmers in Section 4. Section 5 reports projections of future yields based on our spatially flexible approach. Section 6 concludes.

## 2 Empirical Approach

We first introduce our econometric model of a spatiotemporally varying relationship between climate and agriculture and then discuss how it nests more traditional approaches as special cases.

Let us begin with the conventional formulation of a reduced-form relationship between an agricultural outcome $y_{it}$ (e.g., the logarithm of crop yield in our paper) and strictly exogenous weather variables $\mathbf{z}_{it}$ in county $i$ in year $t$:

$$y_{it} = \alpha + \boldsymbol{\beta}'\mathbf{z}_{it} + \mu_i + \epsilon_{it} \qquad \forall\ i = 1, \ldots, n;\ t = 1, \ldots, T, \tag{1}$$

where $\alpha$ is the common intercept term, $\boldsymbol{\beta}$ is a vector of coefficients measuring sensitivity of the mean of agricultural outcome to changes in $\mathbf{z}$, $\mu_i$ captures unobservable county-level heterogeneity, and $\epsilon_{it}$ is an *i.i.d.* noise with $\mathbb{E}\left[\epsilon_{it}|\mathbf{z}_{i1}, \ldots, \mathbf{z}_{iT}, \mu_i\right] = 0$.

Arguably, the popularity of the above panel-data specification in the empirical climate economics literature is mainly driven by its ability to control for unobserved correlated confounders via unit fixed effects, thereby mitigating the omitted variable bias concerns when seeking to identify "average treatment effects on the treated" via $\boldsymbol{\beta}$. However, a key feature of model (1) and its typical variants is that they posit the mean yield-climate relationship that is fixed across space (and over time, but let us abstract away from the latter for now). They also implicitly assume that cross-county heterogeneity in this relationship—say, due to the differential soil quality and other geotopographic factors—is strictly neutral and thus can be fully controlled for via additively separable fixed effects $\{\mu_i\}$. However, given the inherent importance of geography for both climate and agriculture, location may also influence marginal effects of $\mathbf{z}_{it}$ on crop yields. That is, in practice, local heterogeneity is likely *non-neutral*, mediating the yield-climate relationship by shifting not only the intercept but also slopes. In the latter case, ignoring spatial heterogeneity in slopes may jeopardize identification of even the average causal effects of climate via $\boldsymbol{\beta}$ in space-invariant models such as (1).

To fix ideas, consider the mean yield-climate relationship with non-neutral local heterogeneity:

$$y_{it} = \alpha + \underbrace{\left[\boldsymbol{\beta} + \boldsymbol{b}_i\right]'}_{\boldsymbol{\beta}_i}\mathbf{z}_{it} + \mu_i + \epsilon_{it} = \alpha + \boldsymbol{\beta}'\mathbf{z}_{it} + \mu_i + \left(\boldsymbol{b}_i'\mathbf{z}_{it} + \epsilon_{it}\right), \tag{2}$$

where $\boldsymbol{b}_i$ is cross-unit spatial heterogeneity in slopes. From the second equality, it is evident that a model ignoring spatial variation in slopes would suffer from an omitted time-varying confounder $\boldsymbol{b}_i'\mathbf{z}_{it}$ that no standard fixed-effects transformation can remove. Given the naturally expected correlation between spatial heterogeneity $\boldsymbol{b}_i$ and local weather $\mathbf{z}_{it}$ (and very likely $\mu_i$ too), the strict exogeneity of $\mathbf{z}_{it}$ necessary to identify $\boldsymbol{\beta}$ in a panel-data setup would be violated, viz., $\mathbb{E}\left[\boldsymbol{b}_i'\mathbf{z}_{it} + \epsilon_{it}|\mathbf{z}_{i1},\ldots,\mathbf{z}_{iT},\mu_i\right] = \mathbb{E}\left[\boldsymbol{b}_i|\mathbf{z}_{i1},\ldots,\mathbf{z}_{iT},\mu_i\right]'\mathbf{z}_{it} \neq \mathbf{0}$. With that in mind, in this paper, we therefore aim to explicitly accommodate non-neutral cross-location heterogeneity in climate effects on agriculture.

## 2.1 Spatiotemporally Varying Coefficient Model with Fixed Effects

Since fixed-effects estimation of panel-data models relies on a year-to-year within-county variation, even if they were well-identified, the $\boldsymbol{\beta}_i$ slopes in (2) would reflect sensitivity of crop yields to the annual *weather* variation instead of the long-run climate change (see Burke and Emerick, 2016; Blanc and Schlenker, 2017; Chen and Gong, 2021). Given that it is the latter which is the object of real interest, Burke and Emerick (2016) have suggested the idea of modeling the yield-climate relationship using longer-run averages over two separate subperiods, with the rationale being that the long-difference regression leveraging exogenous cross-county variation in long-range temporal changes of local averages can identify marginal effects of *climate* change on yields. In what follows, we too adopt this modeling paradigm but generalize it to allow both spatial and temporal—that is, *spatiotemporal*—heterogeneity in marginal effects, which we accomplish by allowing regression parameters to vary across county locations and over time subperiods.

Splitting the sample period $1,\ldots,T$ into a finite set of mutually exclusive multi-year subperiods $\mathbb{T} = \{a,b,c,\ldots\}$ and letting $s_i$ denote the time-invariant location of county $i$, we arrive at the following generalization of (1):

$$y_{it} = \sum_{\tau\in\mathbb{T}} \alpha_\tau(s_i)\mathbb{1}(t\in\tau) + \sum_{\tau\in\mathbb{T}} \boldsymbol{\beta}_\tau(s_i)'\mathbb{1}(t\in\tau)\mathbf{z}_{it} + \mu_i + \epsilon_{it} \qquad \forall\ i=1,\ldots,n;\ t=1,\ldots,T, \tag{3}$$

where $\{\mathbb{1}(t\in\tau);\ \tau\in\mathbb{T}\}$ is a series of subperiod indicator variables, and all parameters are modeled as smooth nonparametric subperiod-specific functions of the county's geographic location. Thus, our model captures a more flexible relationship between climate and agriculture that can vary both temporally (over subperiods $\tau$) and spatially (between county locations $s_i$).[4] By incorporating geographic information into the model, we obtain parameters that differ between counties. This provides an indirect way to control for observed and unobserved cross-county local heterogeneity (such as different soil quality, institutions, regulations,

[4]While fully nonparametric in the spatial dimension, our model is, in effect, piece-wise linear in the time dimension. We choose such a specification in part because allowing parameters to also be nonparametric functions of time would necessitate the invocation of large-$T$-large-$n$ asymptotics for consistency which is impractical in studies like ours given that $n \gg T$.

and farming practices) that mediates climate effects on agricultural productivity. As such, county-level heterogeneity in (3) is no longer restricted to be additively separable.

Of note, by virtue of modeling cross-county differences as an explicit *smooth* function of the county's location, we are able to parsimoniously accommodate the contiguity/clustering of local heterogeneity across space that naturally arises due to the geography of climate and topography of land. Thus, the cross-county heterogeneity in the yield-climate relationship that our formulation is able to identify is unambiguously "spatial." This is distinct from Butler and Huybers's (2013) and Keane and Neal's (2020) alternative approaches to modeling cross-county heterogeneity as purely "cross-sectional" with no spatial structure, which is akin to just letting coefficients be $\boldsymbol{\beta}_i$ as in (2) or $\boldsymbol{\beta}_{it}$ if one were to extend (2) to also incorporate time heterogeneity. In our case, spatiotemporally varying marginal effects are essentially regularized as $\boldsymbol{\beta}_{it} \equiv \boldsymbol{\beta}_\tau(s_i)$ which smoothly—as opposed to arbitrarily—vary with space across counties.

Averaging (3) over all years in a subperiod $\tau$, we obtain a long-run average relationship between mean crop yields and climate (i.e., average weather over years):

$$\overline{y}_{i\tau} = \alpha_\tau(s_i) + \boldsymbol{\beta}_\tau(s_i)'\overline{\mathbf{z}}_{i\tau} + \mu_i + \overline{\epsilon}_{i\tau} \qquad \forall\ i = 1,\ldots,n;\ \tau = a,b,c,\ldots,\mathbb{T}, \tag{4}$$

where $\overline{x}_{i\tau} = \sum_{t\in\tau} x_{it} \big/ \sum_t \mathbb{1}(t \in \tau)$ for any $x$, and all parameters are period- and location-specific, in effect, making them vary at the observation level. The intercept $\alpha_\tau(s_i)$ captures a local climate-neutral but time-varying contribution of the county's location-specific factors on mean crop yield. Slope parameters $\boldsymbol{\beta}_\tau(s_i)$ measure a local effect of climate on the mean crop yield in period $\tau$ mediated by *non-additive* spatial heterogeneity, and $\mu_i$ represents the remaining additive components of time-invariant county unobservables.

Altogether, a nontrivial distinction between (4) and its analogue derived from standard models akin to (1) is that yield sensitivity to climate variation is no longer constant over time and across space. This is a critical generalization because it accommodates the potential for (mal)adaptation to climate change and, importantly, expressly allows it to be of a heterogeneous degree across different regions. Namely, differencing (4) over two non-adjacent subperiods, say $a$ and $c$, with $a$ being the earlier period, we obtain a "long-differenced" relationship between the mean yield and climate:

$$\Delta\overline{y}_{i(c,a)} = \underbrace{\left[\alpha_c(s_i) - \alpha_a(s_i)\right]}_{\alpha^*_{(c,a)}(s_i)} + \boldsymbol{\beta}_a(s_i)'\Delta\overline{\mathbf{z}}_{i(c,a)} + \underbrace{\left[\boldsymbol{\beta}_c(s_i) - \boldsymbol{\beta}_a(s_i)\right]}_{\boldsymbol{\beta}^*_{(c,a)}(s_i)}{}'\,\overline{\mathbf{z}}_{ic} + \Delta\overline{\epsilon}_{i(c,a)} \quad \forall\ i = 1,\ldots,n, \tag{5}$$

where $\Delta\overline{x}_{i(c,a)} = \overline{x}_{ic} - \overline{x}_{ia}$ for any variable $x$, and the newly defined $\alpha^*_{(c,a)}(s_i) \equiv \alpha_c(s_i) - \alpha_a(s_i)$ and $\boldsymbol{\beta}^*_{(c,a)}(s_i) \equiv \boldsymbol{\beta}_c(s_i) - \boldsymbol{\beta}_a(s_i)$ respectively measure local changes in the intercept and slope functions between periods $a$ and $c$. Therefore, by identifying the change in sensitivity of the $i$th county's mean crop yields to climate variation in the longer run, the slopes $\boldsymbol{\beta}^*_{(c,a)}(s_i)$ indirectly provide us with the information about (mal)adaptation to climate change by local agriculture: a decrease (resp., increase) in sensitivity of yields to harmfully excessive heat would indicate adaptation (resp., maladaptation). In our model (5), such an adaptation is explicitly allowed to vary spatially, reflective of heterogeneous local conditions. Although we ought to emphasize that, given our reduced-form formulation of the yield-climate relationship, one is to interpret $\boldsymbol{\beta}^*_{(c,a)}(s_i)$ as capturing the *net cumulative* effect of all and any various adaptive methods used by farmers.

**Nested Specifications.** Our flexible model constitutes a semiparametric generalization of the popular time-and-location-invariant "long differences" approach by Burke and Emerick (2016) and its recent time-varying extension by Yu et al. (2021). In fact, our spatiotemporally varying model in (5) nests these two as special cases. When $\alpha_\tau(s_i) = \alpha$ and $\boldsymbol{\beta}_\tau(s_i) = \boldsymbol{\beta}$ are restricted for all $\tau$ and $s_i$, it collapses to the Burke and Emerick (2016) specification:

$$\Delta\overline{y}_{i(c,a)} = \boldsymbol{\beta}'\Delta\overline{\mathbf{z}}_{i(c,a)} + \Delta\overline{\epsilon}_{i(c,a)} \qquad \forall\ i = 1,\ldots,n, \tag{6}$$

in which slopes are both spatially and temporally invariant and thus constant.

If one were to "fix" the yield-climate relationship only in the spatial dimension by having $\alpha_\tau(s_i) = \alpha_\tau$ and $\boldsymbol{\beta}_\tau(s_i) = \boldsymbol{\beta}_\tau$ for all $s_i$, our model would then reduce to a time-varying specification à la Yu et al. (2021), in which slopes may change over time but are restricted to be common to all locations:

$$\Delta\overline{y}_{i(c,a)} = \alpha^*_{(c,a)} + \boldsymbol{\beta}'_a\Delta\overline{\mathbf{z}}_{i(c,a)} + \boldsymbol{\beta}^{*\prime}_{(c,a)}\overline{\mathbf{z}}_{ic} + \Delta\overline{\epsilon}_{i(c,a)} \qquad \forall\ i = 1,\ldots,n, \tag{7}$$

where $\alpha^*_{(c,a)} \equiv \alpha_c - \alpha_a$ and $\boldsymbol{\beta}^*_{(c,a)} \equiv \boldsymbol{\beta}_c - \boldsymbol{\beta}_a$.

It may also be of interest to consider a third special case nested within our model, namely, a spatially varying but time-invariant coefficient specification that (5) simplifies to when $\alpha_\tau(s_i) = \alpha(s_i)$ and $\boldsymbol{\beta}_\tau(s_i) = \boldsymbol{\beta}(s_i)$ for all time periods $\tau$. In such an instance, one arrives at a spatially varying extension of the Burke and Emerick (2016) specification:

$$\Delta\overline{y}_{i(c,a)} = \boldsymbol{\beta}(s_i)'\Delta\overline{\mathbf{z}}_{i(c,a)} + \Delta\overline{\epsilon}_{i(c,a)} \qquad \forall\ i = 1,\ldots,n, \tag{8}$$

as can be easily seen by comparing (8) to (6).

On a final note, our spatially varying approach can also be applied to extend the more traditional fixed-effects estimator à la Schlenker and Roberts (2009); see Appendix A for details.

## 2.2 Estimation and Inference

Given our semiparametric functional-coefficient specification of the reduced-form relationship between mean crop yields and climate, we estimate our model in long differences given in (5) via *local* least squares. We employ local-constant kernel fitting. Owing to the time-invariance of smoothing location variable $s_i$, for estimation purposes this long-difference-transformed specification is a cross-sectional varying-coefficient model with a well-known asymptotic behavior (see Li et al., 2002; Li and Racine, 2007, 2010).

Parameters of interest are the unknown nonparametric $s_i$-location-specific coefficients $\boldsymbol{\Theta}(s_i) = [\alpha^*_{(c,a)}(s_i), \boldsymbol{\beta}_a(s_i)', \boldsymbol{\beta}^*_{(c,a)}(s_i)']'$ in (5). Assuming that these coefficient functions are smooth and twice continuously differentiable in the neighborhood of $s$, we can approximate parameter functions $\boldsymbol{\Theta}(s_i)$ at points $s_i$ in the vicinity of location $s$ using a local constant: $\boldsymbol{\Theta}(s_i) \approx \boldsymbol{\Theta}(s)$. Therefore, for locations $\{s_i\}$ close to $s$ such that $|s_i - s| = o(1)$, a spatially-varying long-differenced mean yield-climate relationship in (5) is approximated via

$$\Delta\overline{y}_{i(c,a)} \approx \alpha^*_{(c,a)}(s) + \boldsymbol{\beta}_a(s)'\Delta\overline{\mathbf{z}}_{i(c,a)} + \boldsymbol{\beta}^*_{(c,a)}(s)'\overline{\mathbf{z}}_{ic} + \Delta\overline{\epsilon}_{i(c,a)}, \tag{9}$$

which, given the quasi-random strict exogeneity of climate variation, can be consistently estimated using locally weighted least squares under the standard regularity conditions. The associated kernel estimator is

$$\widehat{\boldsymbol{\Theta}}(s) = \left[\sum_i \overline{\mathbf{x}}_{i(c,a)}\overline{\mathbf{x}}'_{i(c,a)}\mathbb{K}_h(s_i, s)\right]^{-1} \sum_i \overline{\mathbf{x}}_{i(c,a)}\Delta\overline{y}_{i(c,a)}\mathbb{K}_h(s_i, s), \tag{10}$$

where $\overline{\mathbf{x}}_{i(c,a)} = [1, \Delta\overline{\mathbf{z}}'_{i(c,a)}, \overline{\mathbf{z}}'_{ic}]'$ is a vector of regressors. A product kernel $\mathbb{K}_h(s_i, s) = K\left(\frac{s_{1i}-s_1}{h_1}\right) \times K\left(\frac{s_{2i}-s_2}{h_2}\right)$ weights each long-differenced county $i$ on the basis of closeness of its geographic coordinates (i.e., longitude and latitude) $s_i = (s_{1i}, s_{2i})$ to those of the location $s$, with $K(\cdot)$ being a kernel weighting function, $s_1$ and $s_2$ respectively denoting the longitude and latitude of location $s$, and $h_1$ and $h_2$ being the corresponding bandwidths. These bandwidths control the degree of smoothing and weighting, and $||H|| \to 0$, $n|H| \to \infty$ as $n \to \infty$ where $H = \text{diag}\{h_1, h_2\}$. The kernel $K(\cdot)$ is uniformly bounded, non-negative, symmetric and $\int K(v)dv = 1$; we employ a popular second-order Gaussian kernel.

The estimator in (10) illustrates well the way we explicitly model a contiguous nature of spatial heterogeneity in our framework. Namely, by letting marginal effects of climate depend on the county's location via smooth functions $\boldsymbol{\Theta}(s_i)$, the estimated slope heterogeneity is continuous over space as we estimate these slopes for each county by locally averaging over geographically proximate counties.

Due to its semiparametric nature, computation of the asymptotic variance of estimator in (10) is not as simple and its use in finite samples may also be not as easy to justify. We therefore employ Efron's (1982) bias-corrected bootstrap for statistical inference, which we also use to obtain confidence intervals for functions of $\mathbf{\Theta}(s_i)$, such as the (mal)adaptation index and yield change projections. Details are in Appendix B.

## 3 Data

Annual county-level yield data for corn, soybeans, and cotton over 1958–2019 are obtained from the U.S. Department of Agriculture (USDA) National Agricultural Statistics Service (NASS). We focus only on the rainfed counties east of the 100th Meridian because $i$) rainfed counties respectively account for about 97%, 97%, and 90% of corn, soybean, and cotton production in the U.S. over the sample period, and $ii$) crop production in the western counties is heavily influenced by subsidized irrigation systems. We exclude counties that produce these crops for fewer than two years. Our final data sample includes 1,534 counties for corn, 1,042 counties for soybeans, and 235 counties for cotton. We obtain the longitude and latitude of county centroids from the U.S. Census Bureau.

Historical weather data are from Schlenker and Roberts (2009), who have extended the dataset to 2019.[5] It includes daily total precipitation as well as the maximum and minimum temperatures for 4-km grid cells covering the entire U.S. over the period 1950–2019. Following the convention (e.g., see Schlenker and Roberts, 2009; Burke and Emerick, 2016; Malikov et al., 2020; Yu et al., 2021), we use the growing degree days (GDD) to model a nonlinear relationship between temperature and crop yields. Daily GDD measures the time that crops are exposed to temperatures between the lower and upper thresholds during a specific day, and the annual GDD over the entire growing season is defined as the accumulation of daily GDD over the growing season. Following Burke and Emerick (2016), Yu et al. (2021), and the USDA Economic Research Service (2022), we define the growing season as April 1$^{\text{st}}$ to September 30$^{\text{th}}$ for all three crops.[6]

Schlenker and Roberts (2009) find that temperatures over 29°C, 30°C, and 32°C generate harmful effects on corn, soybean, and cotton production, respectively. Therefore, we set upper boundaries of the GDD calculation for each crop at their respective critical thresholds, with the lower threshold always set at 8°C. We denote this variable as $\text{GDD}_{8-r_0\,^\circ\text{C}}$, where $r_0$ equals 29, 30, and 32 for corn, soybeans, and cotton, respectively, and use it to capture the effects of "normal" temperature on yields. To quantify the overheat effect of high temperatures (and the potential adaptation by farmers to combat it in the face of a warming climate), we use a measure of harmful GDD computed for each crop using temperatures in excess of their respective

[5]The dataset is available at http://www.columbia.edu/ ws2162/links.html.

[6]Economic Research Service (2022) documents that the planting season for cotton in the U.S. is typically from March to June and the harvesting season is from August to December. We use April 1$^{\text{st}}$–September 30$^{\text{th}}$ as a reasonable approximation for its growing season.

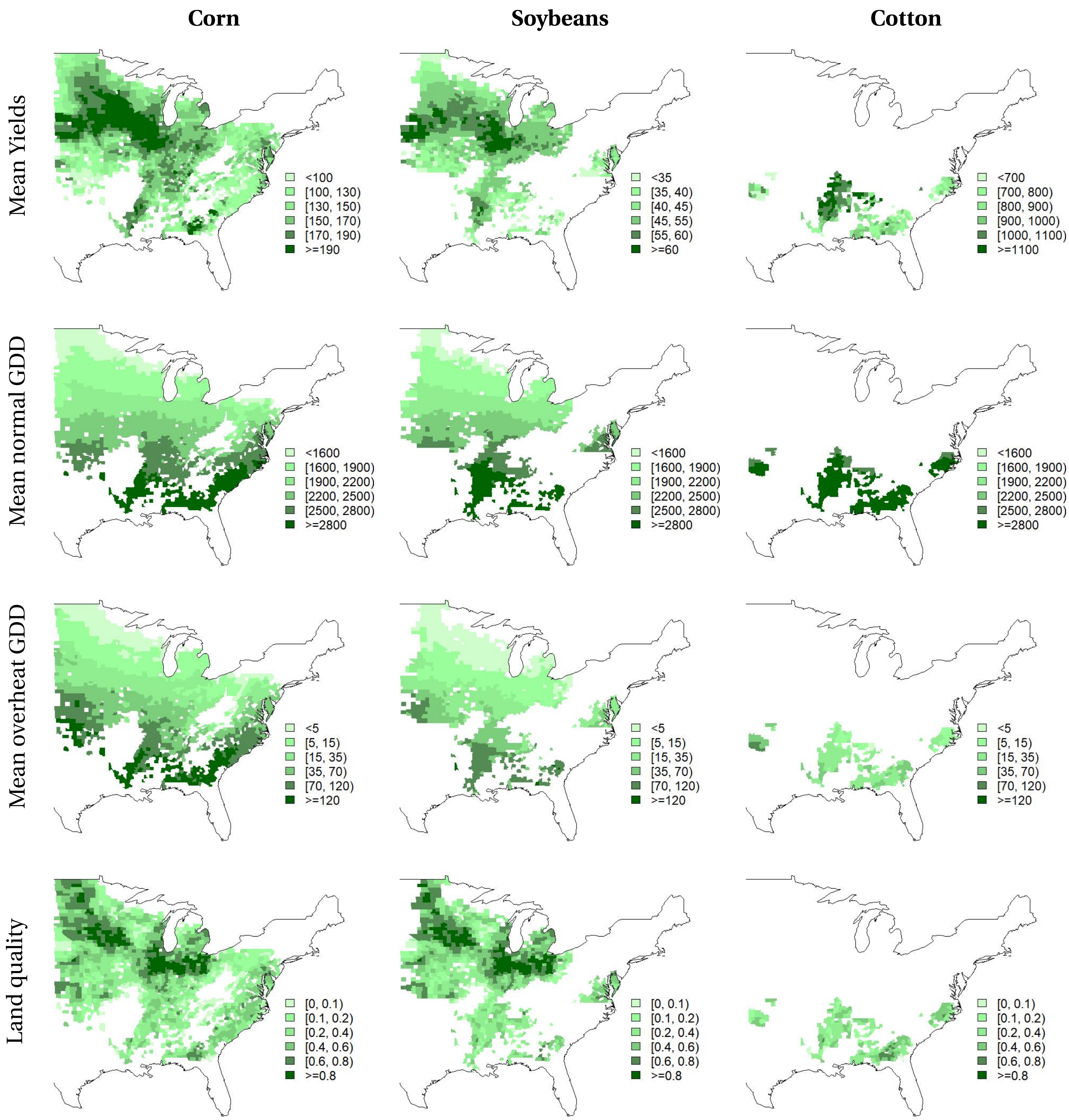


Figure 1. Spatial Distributions of Mean Yields, Mean Normal GDD, Mean Overheat GDD, and Land Quality in 2015–2019

*Notes*: Crop yields are obtained from the USDA NASS and are measured in bushels per acre for corn and soybeans and in pounds per acre for cotton. The historical weather data are obtained from Schlenker and Roberts (2009). Normal GDD measures the time that crops are exposed to temperature between lower and upper thresholds over the entire growing season which is defined to run from April 1 to September 30. We set the lower boundary of the GDD calculation at 8°C and upper boundary for each crop at their respective critical thresholds: 29°, 30°, and 32°C for corn, soybeans, and cotton, respectively. Overheat GDD measures the time that crops are exposed to temperatures in excess of their respective upper thresholds. The land quality is measured by the ratio of LCC 1–2 land (with little or no limitation on crop production) to the total non-developed land in a county. The land capability class (LCC) classification data are obtained from the USDA Natural Resources Conservation Service.

$r_0$ thresholds. We label this overheat GDD variable as $\text{GDD}_{r_0 °\text{C}+}$.

Figure 1 plots maps of the average yield for the three crops and the corresponding GDD and overheat GDD in the last five years of our sample period, 2015–2019 (see the top three rows in the figure). Taking a quick glance at these maps, we already can see the empirical imperative to account for the apparent spatial heterogeneity (and clustering therein) in both yields and climate, when relating agricultural productivity to climate. Spatial differences in crop yields are unarguably related to many local factors and, perhaps more prominently, to the differential soil quality (see the bottom row of Figure 1 for soil quality maps associated with each crop). However, we later show that controlling for these factors via additively separable location (i.e., county) fixed effects is insufficient to fully capture spatial differences in the climate-yield relationship, which motivates a more spatially flexible approach of ours.

Although not the focus of our analysis, we also control for precipitation, which we do along the lines of Burke and Emerick (2016) and Yu et al. (2021). To accommodate potential nonlinearities in precipitation effects on yields, we construct two precipitation-related variables: $i$) total precipitation below a threshold, measuring the severity of water deficiency, and $ii$) total precipitation above the same threshold, measuring the magnitude of water abundance. Appendix C details construction of these precipitation variables and also provides summary statistics of historical yield and weather data (see Table C.1).

Predicted future climate data over 2048–2052 are obtained from the Multivariate Adaptive Constructed Analogs (MACA).[7] We select data from two widely used global climate models. One is the HadGEM2-ES365 model, which tends to predict large temperature increases, and the other is the NorESM1-M model, which predicts small temperature increases. For each one of these climate prediction models, we obtain future climate data predicted under two greenhouse gas representative concentration pathways (RCPs)—RCP4.5 and RCP8.5—that represent medium and the warmest scenarios, respectively. These weather predictions are summarized in Table C.2 in Appendix C.

# 4 Estimates of Spatially Heterogeneous Adaptation to Climate Change

Using our spatiotemporally varying approach, in this section we explore spatial heterogeneity in agricultural adaptation to climate change in the U.S. We first document non-trivial heterogeneity in county-specific estimates of climate sensitivity and adaptation of yields and then explore potential factors that can help ex-

[7]The weblink is https://climate.northwestknowledge.net/MACA/index.php.

Table 1. Estimated Models

| *Model* | *Description* | *Spatially Varying?* | *Time Varying?* | *Estimating Equation* |
|---|---|---|---|---|
| $S_1T_1$ | Our main spatiotemporally varying coefficient model | ✓ | ✓ | eq. (5) |
| $S_1T_0$ | A spatially varying but time-invariant coefficient model | ✓ | × | eq. (8) |
| $S_0T_1$ | A time-varying but spatially invariant coefficient model a là Yu et al. (2021) | × | ✓ | eq. (7) |
| $S_0T_0$ | A both time-and-location-invariant model a là Burke and Emerick (2016) | × | × | eq. (6) |

*Note*: All models are estimated in long differences.

plain the observed variation in local adaptation. Since the first-order threats to agricultural production by a warming climate are arguably posed by the rising temperatures associated with it, we focus on temperature-related variables and, particularly, the overheat GDD.

The estimation is done in long differences for one crop at a time with a log-linear specification.[8] We select two five-year periods that correspond to the beginning and the end of our data sample—the 1958–1962 and 2015–2019 periods—and estimate the long-run average yield-climate relationship using our flexible spatiotemporally varying model in long differences given in (5) and the three restricted specifications in (6) through (8) that it nests.[9] All these models are listed, conveniently labeled, and described in Table 1. Of the four, the first two (spatially varying) models are semiparametric. To estimate them, we need to select the optimal bandwidths that control the degree of spatial smoothing across neighboring counties. Because the county location does not change over time, we employ data-driven leave-one-*location*-out cross-validation to select them (Sun et al., 2009). Our analysis treats geographic coordinates, measured in decimal degrees, as continuous variables because both longitude $s_{1i}$ and latitude $s_{2i}$ are interval variables.

### 4.1 Spatial Heterogeneity in the Agriculture-Climate Relationship

Before proceeding to our main analysis of cross-location heterogeneity in agricultural adaptation (or maladaptation) to a changing climate, we first explore if there is significant spatial heterogeneity in the yield-climate relationship to begin with. To this end, we estimate a restricted version of our spatiotemporally varying model by "fixing" it across time (model $S_1T_0$), and compare its results to those from the standard time-and-location-invariant model $S_0T_0$ by Burke and Emerick (2016). By abstracting away from temporal

[8]All regressions are weighted by the harvested acreage of a corresponding crop in the county in 1960 to facilitate an acreage-based interpretation.

[9]We choose 1958–1962 and 2015–2019 for our main analysis to obtain the longest possible gap between two periods within our data sample. For sensitivity analysis (Appendix E) we further explore results under ten combinations of starting/ending periods for the long-differences models.

Table 2. Estimated Local Sensitivity of Crop Yields to Temperature

| | *Spatially Varying but Time-Invariant* Model $S_1T_0$ | | | | *Space- and Time-Invariant* Model $S_0T_0$ |
|---|---|---|---|---|---|
| | Mean | 1st Qu. | Median | 3rd Qu. | Fixed Coefficient Estimate |
| | | | **Corn** | | |
| $GDD_{8-r_0\,°C}$ | 0.8973 | 0.5469 | 0.7899 | 1.1573 | 0.9756 |
| | (0.8785, 0.911) | (0.5247, 0.5573) | (0.787, 0.7999) | (1.1134, 1.1839) | (0.8774, 1.0611) |
| $GDD_{r_0\,°C+}$ | –3.8424 | –5.6650 | –3.1826 | –1.5844 | –4.2546 |
| | (–3.9699, –3.8006) | (–5.9469, –5.4658) | (–3.3438, –2.9957) | (–1.8028, –1.4757) | (–4.7949, –3.7079) |
| | | | **Soybeans** | | |
| $GDD_{8-r_0\,°C}$ | 0.6067 | 0.4542 | 0.5758 | 0.7429 | 0.6245 |
| | (0.5662, 0.6358) | (0.4182, 0.4953) | (0.5167, 0.6045) | (0.7038, 0.785) | (0.5476, 0.6822) |
| $GDD_{r_0\,°C+}$ | –4.2763 | –6.1139 | –3.9924 | –2.2202 | –3.9847 |
| | (–4.7814, –4.0539) | (–6.7654, –5.8597) | (–4.6785, –3.3023) | (–2.5185, –1.7077) | (–4.6936, –3.1745) |
| | | | **Cotton** | | |
| $GDD_{8-r_0\,°C}$ | 0.6160 | 0.5463 | 0.6000 | 0.6722 | 0.5926 |
| | (0.5782, 0.6475) | (0.5141, 0.5780) | (0.5768, 0.6646) | (0.6011, 0.7274) | (0.5356, 0.6368) |
| $GDD_{r_0\,°C+}$ | –2.2830 | –3.1227 | –2.4719 | –1.6842 | –1.5873 |
| | (–2.8088, –1.9695) | (–3.8541, –2.876) | (–2.7769, –1.884) | (–2.4805, –1.1545) | (–2.4287, –0.3338) |

*Notes*: The left panel summarizes point estimates of the responsiveness of crop yields to temperature variation $\boldsymbol{\beta}(s_i) \times 100$ from the spatially varying but time-invariant model $S_1T_0$. The right panel reports their counterparts $\boldsymbol{\beta} \times 100$ from a spatially and temporally invariant model $S_0T_0$. All models control for precipitation variables. The two-sided 95% bias-corrected confidence intervals clustered at the climate division level are in parentheses. For corn, soybeans, and cotton, $r_0$ equals 29, 30, and 32, respectively. The reported point estimates are semi-elasticities interpretable as percentage changes in the mean crop yield per unit change in climate variables. The expanded version of this table that includes estimated sensitivity to precipitation variables is presented in Table G.1 in Appendix G.

changes in climate change effects for the time being, we are able to focus solely on cross-county differences in heat sensitivity of crop yields.

Because model $S_1T_0$ identifies county-specific heat sensitivity, we obtain a distribution of estimated slope parameters $\boldsymbol{\beta}(s_i)$ that measure *local* effects of climate on mean crop yields across all counties in our sample. Table 2 summarizes their point estimates. In the far right column, the table also reports "globally constant" coefficient estimates from the $S_1T_0$ model's spatially invariant analogue, $S_0T_0$, as a benchmark.

The results from our semiparametric model are largely in line with prior studies (e.g., Burke and Emerick, 2016; Keane and Neal, 2020; Malikov et al., 2020; Yu et al., 2021). The exposure to normal temperatures has a positive effect on yields. Cross-county estimates of sensitivity to normal GDD indicate that the exposure to an additional degree-day of normal temperatures leads to a median increase in corn yields of 0.8%, soybean yields of 0.6%, and cotton yields of 0.6%. On the other hand, the exposure to overheat temperatures has an expectedly adverse effect on yields. Our estimates suggest that an additional unit of overheat GDD leads to a median reduction in corn, soybean, and cotton yields by 3.2%, 4%, and 2.5%, respectively.

More importantly, consistent with non-neutral spatial heterogeneity, the estimated $S_1T_0$ model in Table 2 reveals a significant variation among county-specific climate-sensitivity parameters for all three crops. For example, within an interquartile range of local point estimates, the magnitude of sensitivity to overheat GDD changes by 72% (from –5.67 to –1.58) for corn, 64% (from –6.11 to –2.22) for soybeans, and 46% (from –3.12 to –1.68) for cotton. The corresponding within-quartile changes for normal GDD are 112% (from 0.55 to 1.16), 64% (from 0.45 to 0.74), and 23% (from 0.55 to 0.67). We visualize this variability in the yield-climate relationship mediated by spatial heterogeneity in Figure 2 (rows 1 and 3 from the top), which plots histograms of estimated semiparametric county-specific coefficients along with their location-invariant counterparts depicted using vertical lines. Varying estimates of crop responsiveness to GDD and overheat GDD show fairly wide dispersion, which the popular spatially invariant $S_0T_0$ specification is unable to capture by design because it *a priori* imposes a constant-slope restriction.

This significant cross-location heterogeneity in temperature sensitivity of yields can be seen even more clearly from maps in Figure 2 that show geographical distributions of estimated slopes. What is also evident from these maps is that sensitivity to climate is not merely inhomogeneous across counties but it tends to cluster in space. For instance, the bottom-row maps in Figure 2 show that corn and soybean yields in the upper Midwest and North Great Plains are more sensitive to overheat GDD than their counterparts in the southern areas. In fact, Moran's I test overwhelmingly rejects ($p < 0.0001$) the null of no spatial autocorrelation in all parameters for each crop. This indirectly corroborates a *non-neutral* role of local geography in mediating the yield-climate relationship. Imperatively, usual approaches such as a time-and-location-invariant $S_0T_0$ model, which assume that local heterogeneity is climate-neutral and thus can be accounted for via additively separable county fixed effects, are unable to fully capture spatial characteristics of the relationship between yields and climate. Figure G.1 in Appendix G, which plots spatial distributions of residuals (net of county fixed effects) from the $S_0T_0$ model,[10] provides a visualization of the inadequacy of additive fixed effects to fully account for all cross-location heterogeneity. After netting out location effects, the residuals continue to exhibit spatial dependence, which is also confirmed using formal Moran's I tests. At the very least, it implies that one ought to cluster standard errors when doing inference in spatially invariant models. But it is critical to recognize that treating this residual spatial correlation as merely a variance issue would be tantamount to an *untested* assumption that the residual spatial dependence is confined to random shocks. In the context of discussing eq. (2), the estimation of constant slopes $\boldsymbol{\beta}$ would be consistent only if slope heterogeneity is such that $\mathbb{E}\left[\boldsymbol{b}_i|\mathbf{z}_{i1},\ldots,\mathbf{z}_{iT},\mu_i\right]=\mathbf{0}$ which would be as strong and implausible as

[10]Concretely, from the $S_0T_0$ specification, the plotted residuals are computed as $\Delta\overline{y}_{i(c,a)} - \widehat{\boldsymbol{\beta}}'\Delta\overline{\mathbf{z}}_{i(c,a)}$.

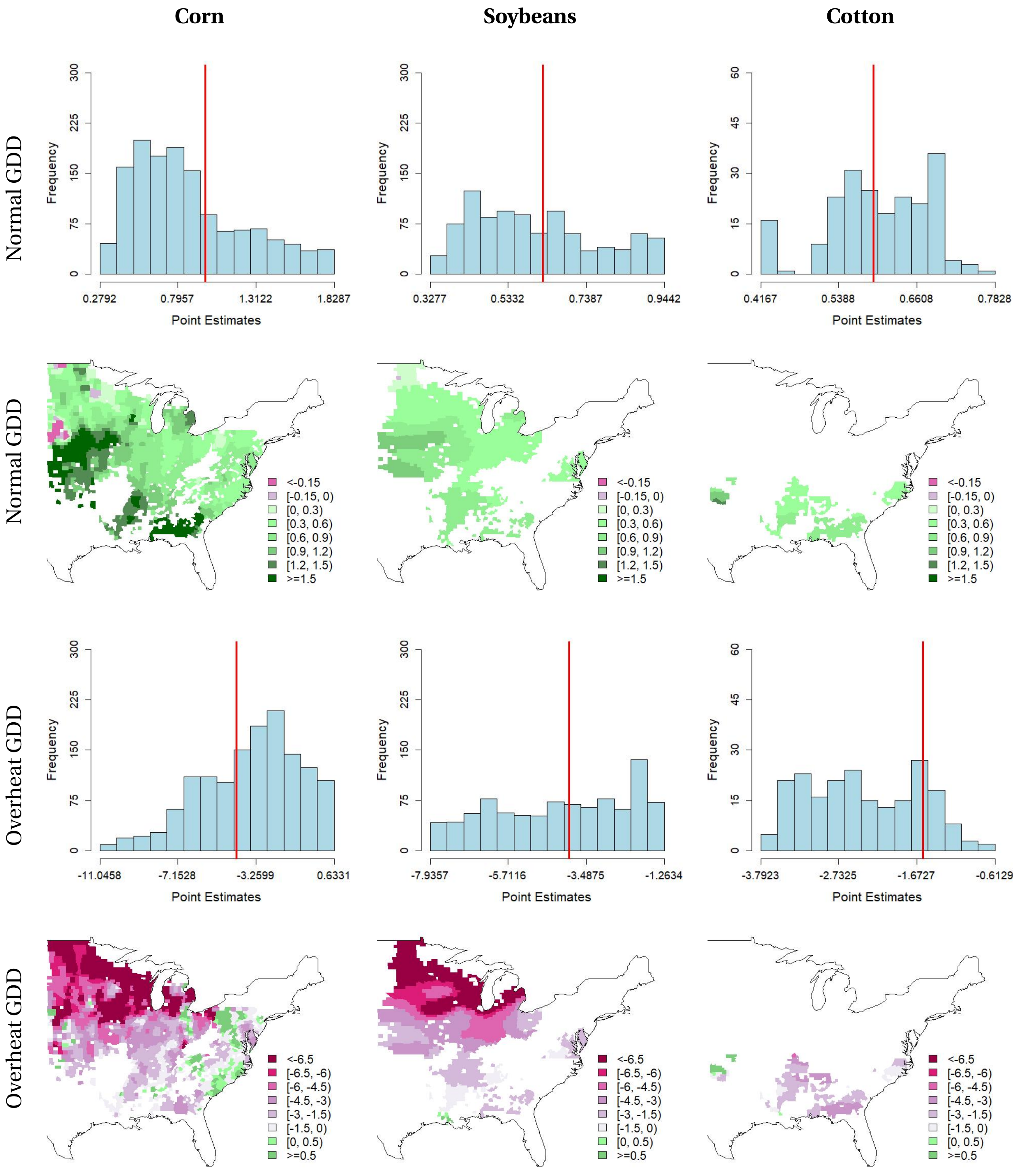


Figure 2. Distributions of Estimated Local Sensitivity of Crop Yields to Temperature

*Notes*: Histograms summarize point estimates of the responsiveness of crop yields to temperature variation, $\boldsymbol{\beta}(s_i) \times 100$, from the spatially varying but time-invariant model $S_1T_0$. Maps plot their spatial distribution. The vertical red lines in the histograms show the counterpart estimates $\boldsymbol{\beta} \times 100$ from a fixed-coefficient, spatially and temporally invariant model $S_0T_0$. All models control for precipitation variables. The plotted point estimates are semi-elasticities interpretable as percentage changes in the mean crop yield per unit change in climate variables.

the assumption that $\mu_i$ were not fixed but random effects.

Although results from the $S_1T_0$ model already provide ample evidence of non-negligible spatial heterogeneity in the relationship between crop yields and climate, we test for both its significance and empirical relevance more formally. First, we rely on Hall et al.'s (2007) result in that local-constant kernel methods, which we employ to estimate spatially varying models, can identify irrelevant regressors via cross-validation procedure. When optimally selected, a large bandwidth parameter would effectively "smooth out" the location variable $s_i$, rendering all parameters in the model globally constant. This provides an indirect *data-driven* method to assess empirical relevance of the county's geographic location in the estimation of climate change effects on agricultural productivity. For the $S_1T_0$ model, cross-validated bandwidths for the longitude and latitude are respectively 60.3 and 36.2 kilometers (km) for corn, 136.9 and 28.7 km for soybeans, and 52.7 and 61 km for cotton.[11] These bandwidths are small relative to the vast geographical area covered in our study (more than 2,200 km from west to east and 2,000 km from south to north), which averts smoothing out of the location, providing strong evidence that county location plays an important role in mediating the yield-climate relationship. Thus, the data reject spatial invariance.

Our spatially varying approach is also supported by Ullah's (1985) goodness-of-fit model specification test which facilitates a joint-hypothesis inference about spatial invariance. The test is essentially a non-parametric F-test that discriminates between a "restricted" time-and-location-invariant $S_0T_0$ specification under the null and a more flexible "unrestricted" spatially-varying $S_1T_0$ specification under the alternative. The test statistic is based on the distance between residual sums of squares from the two specifications: $T_n = (RSS_r - RSS_{ur})/RSS_{ur}$, where $RSS_r$ and $RSS_{ur}$ are restricted and unrestricted sums of squared residuals, respectively. Intuitively, just like an F-test, the test statistic is expected to converge to 0 under the null and is positive under the alternative; hence, the test is one-sided. We approximate the null distribution of $T_n$ via bootstrap by resampling residuals from the restricted specification; the algorithm is provided in Appendix D. With a $p$-value $\leq 0.001$, we confidently reject the null of a location-invariant model for both corn and soybean yields. In the case of cotton, we however fail to reject spatial homogeneity of parameters at the conventional significance levels but do reject it comfortably for our main model that also explicitly incorporates temporal variation in coefficients (more on this later).

[11] To be precise, since geographic coordinates are measured in decimal degrees, the actual bandwidth values for longitude and latitude are 0.543° and 0.326° for corn, 1.230° and 0.258° for soybean, and 0.474° and 0.550° for cotton. For convenience, here we have converted them to km using the 1° = 111km approximation that is valid at the equator.

### 4.2 Local Adaptation to Climate Change

Having established significant cross-location heterogeneity in climate effects on crop yields, we now investigate if there is also spatial heterogeneity in *adaptation* or *maladaptation* to climate change, which can be inferred from changes in temperature sensitivity of yields over time. To this end, we estimate our proposed spatiotemporally varying model $S_1T_1$ which permits coefficients to vary across both time and counties.

Table 3 summarizes our local estimates of the early-period-$a$ temperature sensitivity (the $\beta_a(s_i)$ coefficients) and of *changes* in this sensitivity between period $a$ and the later period $c$ (the $\beta^*_{(c,a)}(s_i)$ coefficients).[12] The earlier-period coefficients can be used as a reference to facilitate interpretation of positive values of $\beta^*_{(c,a)}(s_i)$ as the evidence of adaptation, whereby positive effects on yield in the earlier period become "more positive" and negative effects become "less negative" over time. Analogously, negative values of $\beta^*_{(c,a)}(s_i)$ can be interpreted as capturing maladaptation because they indicate that positive effects on yield in the earlier period become "less positive" and negative effects "more negative."[13] For comparison, the right panel of Table 3 also reports estimates from a location-invariant $S_0T_1$ specification à la Yu et al. (2021).

As in the case of the $S_1T_0$ model, optimal cross-validated bandwidths for location variables in our spatiotemporally varying model are fairly small for all three crops, which is consistent with the reported evidence that geographic location is an empirically relevant variable for measuring agricultural adaptation to climate change.[14] This is further corroborated by a formal test. Using Ullah's (1985) test, we consistently reject the spatially invariant Yu et al. (2021) specification $S_0T_1$ in favor of our more flexible alternative $S_1T_1$ at the 5% significance level for all crops ($p < 0.035$).

Per our proposed model $S_1T_1$, estimates of $\beta^*_{(c,a)}(s_i)$ for normal $\text{GDD}_{8-r_0\,^\circ\text{C}}$ are generally negative whereas estimates of $\beta^*_{(c,a)}(s_i)$ for overheat $\text{GDD}_{r_0\,^\circ\text{C}+}$ are primarily positive. This also holds under the $S_0T_1$ model, particularly for soybeans. However, our model suggests that, on average, $\beta^*_{(c,a)}(s_i)$ for $\text{GDD}_{8-r_0\,^\circ\text{C}}$ is statistically insignificant for corn and cotton yields, with some counties showing maladaptation and some showing adaptation to normal GDD. This finding differs from that of Yu et al. (2021), who find that U.S. corn displayed statistically significant maladaptation to normal GDD in the past few decades. Given the statistical insignificance of $\beta^*_{(c,a)}(s_i)$ for $\text{GDD}_{8-r_0\,^\circ\text{C}}$ in our main model $S_1T_1$ and the potential for large detrimental

[12] Estimates of a full set of parameters, including local sensitivity to precipitation, are reported in Table G.2 in Appendix G.

[13] In the context of global warming this differentiation of adaptation and maladaptation is reasonable because, as agriculture is exposed to an increasing amount of normal GDD and overheat GDD, adaptation should mitigate negative effects and enlarge positive effects of temperature. If it were global cooling, definitions of adaptation and maladaptation would be the opposite.

[14] For our main model $S_1T_1$, when converted to kilometers, optimal bandwidths for longitude and latitude are respectively equal to 315.1 and 227.7 km for corn, 294.5 and 308.5 km for soybean, and 366.2 and 477.8 km for cotton.

Table 3. Estimated Time-Varying Local Sensitivity of Crop Yields to Temperature

| | *Spatially and Temporally Varying* Model $S_1T_1$ | | | | *Spatially Invariant* Model $S_0T_1$ |
|---|---|---|---|---|---|
| | Mean | 1st Qu. | Median | 3rd Qu. | Fixed Point Estimate |
| **Corn** | | | | | |
| $\beta_a(s_i)$ for $\text{GDD}_{8-r_0{}^\circ\text{C}}$ | –0.0024 | –0.0577 | –0.0240 | 0.0591 | 0.1105 |
| | (–0.0422, 0.0155) | (–0.1045, –0.0259) | (–0.0574, –0.0103) | (0.0238, 0.0777) | (0.0555, 0.1701) |
| $\beta_a(s_i)$ for $\text{GDD}_{r_0{}^\circ\text{C}+}$ | –0.6076 | –1.267 | –0.4927 | –0.0250 | –1.5653 |
| | (–0.6606, –0.4473) | (–1.4114, –0.8868) | (–0.6357, –0.2094) | (–0.1326, 0.2383) | (–1.9274, –1.2595) |
| $\beta^*_{(c,a)}(s_i)$ for $\text{GDD}_{8-r_0{}^\circ\text{C}}$ | –0.0064 | –0.0846 | 0.0050 | 0.0587 | –0.0704 |
| | (–0.0147, 0.0128) | (–0.1010, –0.0680) | (–0.0098, 0.0360) | (0.0451, 0.0870) | (–0.0954, –0.0457) |
| $\beta^*_{(c,a)}(s_i)$ for $\text{GDD}_{r_0{}^\circ\text{C}+}$ | 0.4820 | 0.0399 | 0.3311 | 0.8936 | 1.1666 |
| | (0.3762, 0.5080) | (–0.1682, 0.1097) | (0.1839, 0.3631) | (0.7152, 0.9444) | (0.975, 1.3637) |
| **Soybeans** | | | | | |
| $\beta_a(s_i)$ for $\text{GDD}_{8-r_0{}^\circ\text{C}}$ | 0.0724 | 0.0214 | 0.0695 | 0.1219 | 0.0808 |
| | (0.0343, 0.1149) | (–0.0164, 0.0771) | (0.0270, 0.1204) | (0.0468, 0.1696) | (0.0228, 0.1354) |
| $\beta_a(s_i)$ for $\text{GDD}_{r_0{}^\circ\text{C}+}$ | –1.1141 | –1.5248 | –0.9711 | –0.7456 | –1.3388 |
| | (–1.4228, –0.8325) | (–2.1129, –1.1609) | (–1.2043, –0.6677) | (–1.0054, –0.4841) | (–1.7646, –0.9705) |
| $\beta^*_{(c,a)}(s_i)$ for $\text{GDD}_{8-r_0{}^\circ\text{C}}$ | –0.0384 | –0.0620 | –0.0348 | –0.0129 | –0.0555 |
| | (–0.0493, –0.0288) | (–0.0820, –0.0502) | (–0.0414, –0.0216) | (–0.0219, 0.0020) | (–0.0741, –0.0355) |
| $\beta^*_{(c,a)}(s_i)$ for $\text{GDD}_{r_0{}^\circ\text{C}+}$ | 0.6042 | 0.3171 | 0.5195 | 0.8801 | 0.8450 |
| | (0.4530, 0.7902) | (0.1080, 0.4543) | (0.3419, 0.6069) | (0.7191, 1.2066) | (0.5787, 1.0933) |
| **Cotton** | | | | | |
| $\beta_a(s_i)$ for $\text{GDD}_{8-r_0{}^\circ\text{C}}$ | 0.1183 | 0.1416 | 0.1538 | 0.1565 | 0.0972 |
| | (0.0498, 0.1681) | (0.0955, 0.2123) | (0.1021, 0.2272) | (0.0950, 0.2140) | (–0.0046, 0.2061) |
| $\beta_a(s_i)$ for $\text{GDD}_{r_0{}^\circ\text{C}+}$ | –0.3750 | –0.6955 | –0.3906 | –0.2985 | –0.1875 |
| | (–0.8832, 0.0435) | (–1.3843, –0.2443) | (–0.8659, 0.0915) | (–0.8226, 0.1645) | (–0.9508, 0.6718) |
| $\beta^*_{(c,a)}(s_i)$ for $\text{GDD}_{8-r_0{}^\circ\text{C}}$ | –0.0245 | –0.0445 | –0.0239 | –0.0067 | –0.0445 |
| | (–0.044, 0.0108) | (–0.0683, –0.0047) | (–0.0457, 0.0143) | (–0.0402, 0.0285) | (–0.0791, –0.0062) |
| $\beta^*_{(c,a)}(s_i)$ for $\text{GDD}_{r_0{}^\circ\text{C}+}$ | 0.1707 | –0.0135 | 0.1196 | 0.3655 | 0.4437 |
| | (–0.2053, 0.5282) | (–0.5472, 0.5402) | (–0.3164, 0.4093) | (–0.0037, 0.6182) | (0.0612, 0.8795) |

*Notes*: The left panel summarizes point estimates of the responsiveness of crop yields to temperature variation in the early period $\boldsymbol{\beta}_a(s_i) \times 100$ and its *change* over time $\boldsymbol{\beta}^*_{(c,a)}(s_i) \times 100$ from the spatiotemporally varying model $S_1T_1$. The right panel reports their counterparts $\boldsymbol{\beta}_a \times 100$ and $\boldsymbol{\beta}^*_{(c,a)} \times 100$ from a spatially-fixed but temporally varying model $S_0T_1$. All models control for precipitation variables. Two-sided 95% bias-corrected confidence intervals clustered at the climate division level are in parentheses. For corn, soybeans, and cotton, $r_0$ equals 29, 30, and 32, respectively. The reported point estimates are semi-elasticities interpretable as percentage changes in the mean crop yield per unit change in climate variables. The expanded version of this table that includes estimated sensitivity to precipitation variables is presented in Table G.2 in Appendix G.

impacts of overheat on crops (see Wagner and Schlenker, 2022), in what follows we focus our discussion on the (mal)adaptation to *overheat* GDD.

Our spatially varying estimates in Table 3 show that, as expected, the sensitivity of crop yields to overheat GDD in the early period (i.e., $\beta_a(s_i)$ for $\text{GDD}_{r_0\,^\circ\text{C}+}$) is negative, suggesting that in 1958–1962 mean crop yields would fall in response to an increase in overheat temperatures. Moreover, we find that temporal changes in overheat sensitivity are positive and statistically significant—albeit, not everywhere—and that magnitudes of these changes vary non-negligibly across counties, indicating that adaptation to climate change *is* occurring but it is *not* spatially homogeneous. Magnitudes of adaptation from a location-invariant specification are much larger than the corresponding mean/median estimates from our spatiotemporally varying model, suggesting that approaches incapable of accommodating spatial heterogeneity in slopes may overestimate the degree of adaptation.

To further explore the geography of adaptation, we include histograms and maps of our local adaptation estimates in Figure 3. Also included in the figure is a breakdown of counties based on the statistical significance (at the 5% level) of their historical adaptation to excessive heat. While the $\text{S}_0\text{T}_1$ specification finds that overheat adaptation was statistically significant for all three crops including cotton, this is not quite the case based on our more flexible approach. Not only do we find that heat adaptation by cotton farmers is insignificant on average, it is actually not different from zero in 77% of producing counties.[15] For corn and soybeans, the evidence of local adaptation is much stronger, however. Although still not uniformly across all locations, we find that 54% and 75% of counties, respectively, experienced a statistically significant decrease in heat sensitivity, helping farmers adapt to a warming climate. Geographically, these adapting counties are mainly located in the Northern Great Plains and Upper Midwest (see maps in Figure 3). Therefore, our findings on agricultural adaptation differ from "average" estimates in both Yu et al. (2021), who find ubiquitous adaptation, and Burke and Emerick (2016), who find no adaptation.

To get a better feel of the extent of adaptation by farmers, we use our estimates of local adaptation $\beta^*_{(c,a)}(s_i)$ to compute two supplementary measures of adaptation which have a more concrete interpretation. First, we calculate a percentage change in sensitivity of crop yields to overheat temperatures between the two periods via $\text{sign}\{\beta^*_{(c,a)}(s_i)\} \times |\beta^*_{(c,a)}(s_i)/\beta_a(s_i)| \times 100\%$, where the ratio of $\beta^*_{(c,a)}(s_i)$ to $\beta_a(s_i)$ provides the magnitude of a proportional change in heat sensitivity, and $\beta^*_{(c,a)}$ signs it. Given the adverse effect of overheat on yields, when positive this measure corresponds to a decrease in the magnitude of a negative

[15] This may be because high yield is not the only goal for cotton farmers. Other important factors that determine cotton quality and thus price, such as fiber length, need to be considered as well in the cotton production.

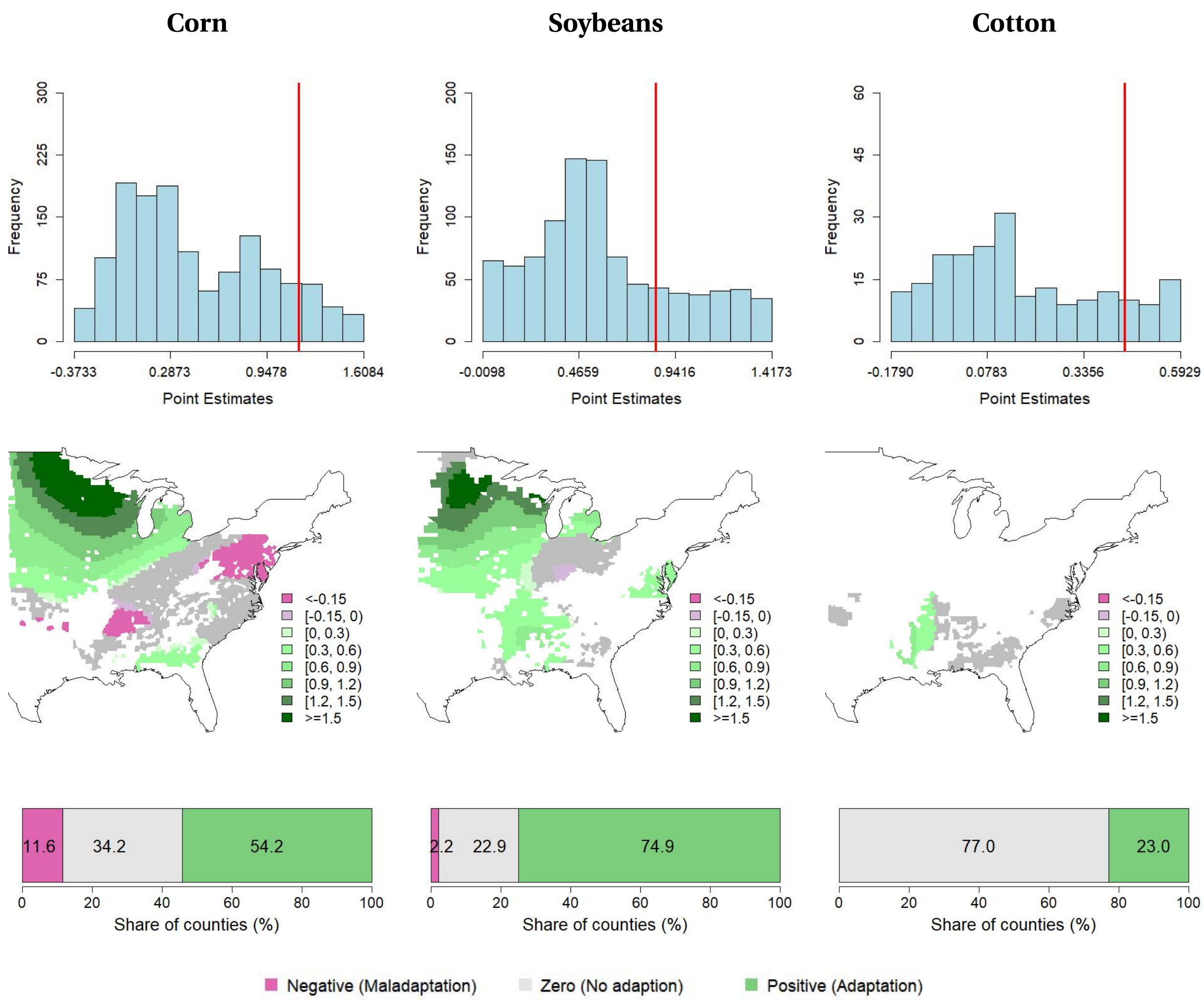


Figure 3. Estimated Temporal Changes in Local Sensitivity of Crop Yields to Overheat Temperatures

*Notes:* Histograms summarize point estimates of the *change* in responsiveness of crop yields to overheat GDD over time, $\beta^*_{(c,a)}(s_i) \times 100$, from the spatiotemporally varying model $S_1T_1$. Maps plot their spatial distribution: regardless of their magnitude or sign, all statistically insignificant estimates are shown using the same shade of gray. Barplot reports the breakdown of counties based on the statistical significance of point estimates of $\beta^*_{(c,a)}(s_i)$. "Negative" if statistically significant but has a negative sign; "zero" if statistically insignificant; and "positive" if the county-specific point estimate is statistically significant at the 5% level and has a positive sign. The vertical red lines in the histograms show the counterpart estimates $\beta^*_{(c,a)} \times 100$ from a spatially-fixed but temporally varying model $S_0T_1$. All models control for precipitation variables. The plotted point estimates are semi-elasticities interpretable as percentage changes in the mean crop yield per unit change in climate variables.

Table 4. Evidence of Local (Mal)Adaptation to Overheat Temperatures

| | *Spatially and Temporally Varying* Model $S_1T_1$ | | | | *Spatially Invariant* Model $S_0T_1$ |
|---|---|---|---|---|---|
| | Weighted Mean | 1st Qu. | Median | 3rd Qu. | Fixed Point Estimate |
| | **Percentage Changes in Local Overheat Sensitivity of Crop Yields** | | | | |
| Corn | 73.29 | 33.39 | 64.14 | 88.81 | 74.53 |
| | (49.25, 79.51) | (–90.4, 48.36) | (49.46, 82.09) | (61.49, 106.05) | (62.11, 89.87) |
| Soybeans | 48.98 | 39.04 | 54.58 | 67.15 | 63.12 |
| | (35.29, 72.47) | (16.12, 52.83) | (42.12, 70.62) | (54.89, 95.35) | (46.04, 84.10) |
| Cotton | 50.85 | 0.80 | 23.75 | 123.52 | 236.60 |
| | (–520.48, 362.27) | (–508.14, 60.17) | (–425.51, 67.83) | (35.26, 596.26) | (75.20, 31501.69) |
| | **Crop Yield Gains due to Local Adaptation (in %)** | | | | |
| Corn | 17.68 | 2.03 | 9.71 | 26.69 | 36.15 |
| | (14.55, 18.53) | (–4.42, 4.60) | (4.77, 10.90) | (16.92, 31.46) | (29.42, 43.43) |
| Soybeans | 10.49 | 2.86 | 9.16 | 19.43 | 18.46 |
| | (6.65, 12.49) | (1.15, 4.39) | (5.68, 11.39) | (13.96, 22.29) | (12.3, 24.51) |
| Cotton | 3.12 | 0.11 | 2.73 | 5.56 | 10.09 |
| | (–5.67, 10.68) | (–11.15, 10.54) | (–5.67, 10.20) | (–1.03, 10.14) | (1.33, 21.00) |

*Notes*: The top left panel summarizes point estimates of the percentage change in responsiveness of crop yields to overheat GDD computed based on the spatiotemporally varying model $S_1T_1$. We calculate it via $\text{sign}\{\beta^*_{(c,a)}(s_i)\} \times |\beta^*_{(c,a)}(s_i)/\beta_a(s_i)| \times 100\%$. The bottom left panel summarizes point estimates of the percentage changes in crop yield due to adaptation to overheat GDD based on the spatiotemporally varying model $S_1T_1$. We calculate it via $\left(\exp\{\beta^*_{(c,a)}(s_i) \times \overline{\text{GDD}}_{r^\circ\text{C}+,ic}\} - 1\right) \times 100\%$. The two right panels reports their counterparts from a spatially-fixed but temporally varying model $S_0T_1$. Weighted mean is calculated using crop acreages in 1960. Two-sided 95% bias-corrected confidence intervals clustered at the climate division level are in parentheses.

responsiveness, indicating adaptation. Second, we scale our local adaptation estimates using each county's average overheat GDD in the later period, viz., $\beta^*_{(c,a)}(s_i) \times \overline{\text{GDD}}_{r_0{}^\circ\text{C}+,ic}$, to obtain the measurement of adaptation in terms of crop yield gains. Unlike the "raw" adaptation estimate $\beta^*_{(c,a)}(s_i)$ that measures a nominal change in the slope of overheat GDD, this one transforms the former into a change in log-yield attributable to a change in heat sensitivity, fixing the climate at period $c$. We convert the change in log-yield to a percentage gain in yields via $\left(\exp\{\beta^*_{(c,a)}(s_i) \times \overline{\text{GDD}}_{r_0{}^\circ\text{C}+,ic}\} - 1\right) \times 100\%$. Both these measures are summarized in Table 4, where we also include their counterparts from a location-invariant $S_0T_1$ specification computed analogously but using geographically constant parameter estimates.

On acreage-weighted average, by 2015–2019 overheat sensitivity of corn and soybean yields decreased significantly—by 73% and 49%, respectively (see the column 'Weighted Mean' in Table 4)—indicating that these crops have become, generally, more heat-resilient due to adaptation. For cotton, as already discussed earlier, adaptation to high temperatures was not as widely prevalent but it did occur in about a quarter of producing locations (see the bottom row in Figure 3). This is particularly notable because the location-invariant model estimates the decline in heat sensitivity of cotton yields at a staggering 237%. In terms

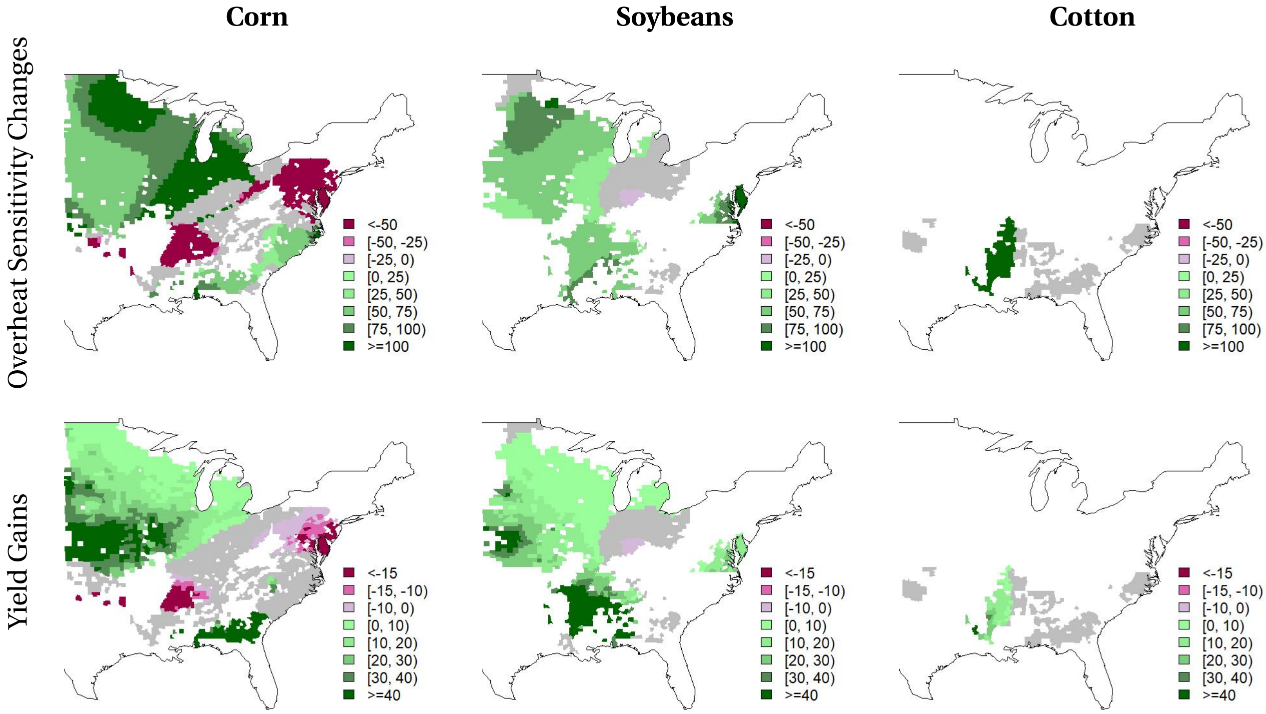


Figure 4. Spatial Distributions of Percentage Changes in Overheat Sensitivity and the Associated Crop Yield Gains due to Local Adaptation or Maladaptation

*Notes*: Maps in the top row plot point estimates of the percentage change in the sensitivity of crop yields to overheat GDD between periods $a$ and $c$. The percentage change is calculated via $\mathrm{sign}\{\beta^*_{(c,a)}(s_i)\} \times |\beta^*_{(c,a)}(s_i)/\beta_a(s_i)| \times 100\%$. Maps in the bottom row plot point estimates of the associated percentage changes in crop yield due to adaptation or maladaptation to overheat GDD. We calculate it via $\big(\exp\{\beta^*_{(c,a)}(s_i)\overline{\mathrm{GDD}}_{r;\,^\circ\mathrm{C}+,ic}\} - 1\big) \times 100\%$. For all maps, calculations are based on estimates from the spatiotemporally varying model $\mathrm{S}_1\mathrm{T}_1$. Regardless of their magnitude or sign, all statistically insignificant (at the 5% level) estimates are shown using the same shade of gray. Green colors indicate statistically significant adaptation, red colors indicate statistically significant maladaptation, and gray color indicates no significant adaptation or maladaptation.

of the yield change due to overheat adaptation, average gains for corn and soybeans were significant and respectively estimated at 17.7% and 10.5%, relative to their 1958–1962 mean levels. Notably, these average yield gains from our model are only about half of their counterparts obtained from a spatially invariant model $\mathrm{S}_0\mathrm{T}_1$ used by Yu et al. (2021).

To explore geographic heterogeneity in the degree of adaptation, consider Figure 4 that plots county-specific estimates of changes in overheat sensitivity (see maps in the top row) and crop yield gains due to local adaptation to overheat (see maps in the bottom row), with statistically insignificant point estimates—regardless of their sign or magnitude—colored using the same shade of gray. Expectedly, the pattern of spatial clustering (as well as the positive/negative delineation) here is similar to that observed for "raw" estimates of local adaptation in Figure 3. For corn, the figure shows that areas with the highest percentage changes in sensitivity to overheat GDD may not necessarily have had the largest yield gains. More specifically, the highest percentage changes tend to have occurred in northern areas whereas the largest yield gains tended to occur in southern areas of the Corn Belt. At least in part, this is because the northern part of the studied region experienced the largest changes in the magnitude of overheat sensitivity (see maps in Figure 3) whereas the southern part of the studied region had the highest values of overheat GDD (see maps in Figure 1). We observe that some areas in a few Midwestern states (e.g., Kansas, Missouri, Nebraska, and Iowa) and Southern states (e.g., Geogia, South Carolina, and Alabama) show the largest yield gains in corn due to adaptation, whereas producers in western Tennessee and northern Mississippi as well as the Northeast region including Pennsylvania and Maryland suffer from a decrease in corn yields due to maladaptation. In the case of soybeans, consistent with our earlier findings, maladaptation to overheat temperatures is practically nonexistent. Significant adaptation occurred in the western part of the Midwest as well as in Mississippi and Arkansas. Lastly, among cotton farmers, statistically significant adaption appears to have been limited mainly to counties in Arkansas, Louisiana, and Mississippi.

**Robustness Analysis.** We examine whether our main findings continue to hold when we long-difference over different periods with different gap widths in Appendix E. The results are qualitatively comparable.

### 4.3 Explaining Spatial Variation in Adaptation

We explore factors and mechanisms that may explain the cross-location variation in adaptation to overheat temperatures. First, we examine the relationship between adaptation and local overheat temperatures. In top-row plots in Figure 5, we study how the change in overheat sensitivity of crop yields, which substantially varies across locations, relates to local intensity of overheating temperatures. For all three crops, we observe that counties experiencing fewer days of excessively high temperatures in period $c$ are the ones that have adapted the most since the earlier period $a$ (relative to locations with much higher mean overheat GDD). Although this finding might at first seem quite counter-intuitive, it is not. Recall that plotted $\beta^*_{(c,a)}(s_i)$ slopes measure a *change* in local overheat sensitivity over time since period $a$. Then, given a naturally diminishing capacity to adapt to high temperatures and the presumed optimality of farmer adaptation behavior, the decline in overheat sensitivity with the intensity of excessive temperatures is consistent with a narrative in which farmers from locations that experienced more overheat in the earlier period $a$ had already adapted more. Consequently, given rising temperatures, locations that were spared from overheat before had the most adaptation to do. As such, adaptive methods become less effective at mitigating marginal damages when overheat GDD is high and increases. This is consistent with arguments in Butler and Huybers (2013)

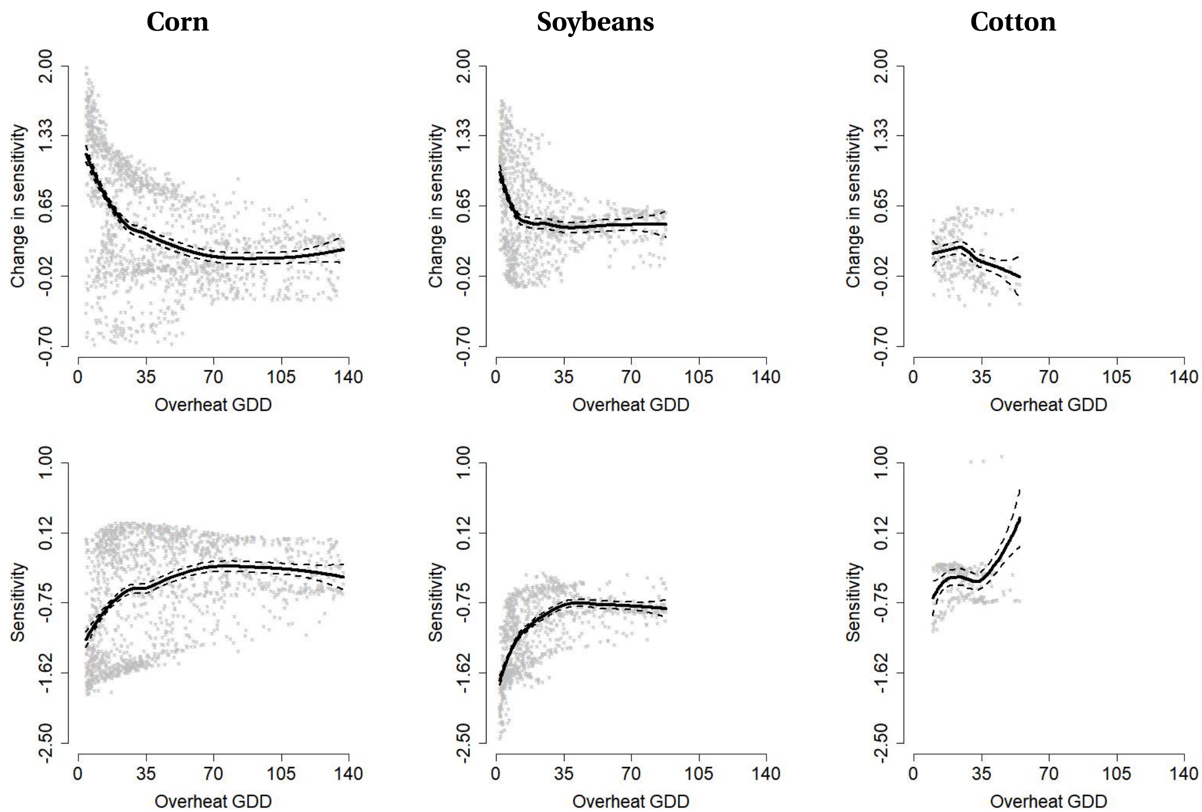


Figure 5. Variation of Local Overheat GDD Adaptation (top row) and Local Overheat GDD Sensitivity (bottom row) across Overheat GDD

*Notes:* The top-row graphs plot point estimates of the *change* in responsiveness of crop yields to overheat GDD between periods $a$ and $c$ (the $\beta^*_{(c,a)}(s_i) \times 100$ parameter) from the spatiotemporally varying model $S_1T_1$ against the mean overheat GDD in each county in period $c$ (i.e., 2015–2019). The bottom-row graphs plot point estimates of the responsiveness of crop yields to overheat GDD in period $a$ (the $\beta_a(s_i) \times 100$ parameter) from the spatiotemporally varying model $S_1T_1$ against the mean overheat GDD in each county in period $a$ (i.e., 1958–1962). Fitted local-linear smoothing mean regressions (solid line) with the corresponding 95% confidence intervals (dashed lines) are superimposed on the scatterplots. To minimize influence of outliers, counties in the bottom or top 5% of the distribution of mean overheat GDD are omitted.

and Keane and Neal (2020) and is also corroborated by our data. Namely, three graphs in the bottom row of Figure 5 plot local overheat sensitivity in period $a$ and show that crop yields in locations with high overheat GDD already had a significantly smaller sensitivity to begin with, presumably because farmers there had already been taking adaptive measures, an argument that can be traced back to Mendelsohn et al. (1994).

Besides overheat temperatures, other factors may also help explain spatial variation in farmers' adaptation, such farming policies, technologies, practices, and natural endowments. In Appendix F, we consider four major aspects that may substantially influence farming practices and outcomes in U.S. agriculture: adoption of genetically engineered (GE) crops, cover crops, crop insurance, and land quality. We find that GE crops, crop insurance, and even land quality, generally, are not predictive of agricultural adaptation, whereas a cross-county variation in cover crop adoption and overheat temperatures does help explain spatial differences in agricultural adaptation. Exploring and attempting to causally identify structural links between these processes should be a promising avenue for future research.

## 5 Projection of Future Crop Yield Changes

In this section, we project expected damages of climate change on U.S. crop yields between the end of our sample period and the mid-21st century. For these projections, we use predicted future weather data from two global climate models—HadGEM2-ES365 and NorESM1-M—under two global warming scenarios: RCP4.5 (mild warming) and RCP8.5 (severe warming). We conduct this projection analysis based on regression results from our flexible $S_1T_1$ model and compare these projections to those based on two existing alternatives: Yu et al.'s (2021) $S_0T_1$ and Burke and Emerick's (2016) $S_0T_0$ specifications. Contrasting projections across models, we can assess practical implications of explicitly allowing for spatiotemporally inhomogeneous historical effects of climate on agricultural production, as opposed to focusing on "average effects," when measuring expected damages of a warming climate in the future.

We use 2015–2019 as the base period (the later period $c$ used in the long-differences estimation for our main results) and 2048–2052 as the future period (labeled $d$) for projections. To compute the future climate change, we difference five-year averages of climate variables between these two periods to obtain $\Delta\bar{\mathbf{z}}_{i(d,c)} = \bar{\mathbf{z}}_{id} - \bar{\mathbf{z}}_{ic}$. Then, to avoid excessive extrapolation and making additional assumptions about U.S. agriculture, we consider a "business as usual" scenario whereby no technological adaptation (i.e., $\boldsymbol{\beta}^*_{(d,c)} = 0$), no climate-neutral technical change (i.e., $\alpha^*_{(d,c)} = 0$), and no relocation of crop production are to occur between the end of our sample period and 2048–2052. To do so, we fix coefficients in the yield-climate relationship at their 2015–2019 values. As such, a projected change in log-yield due to a warming climate in each location $s_i$ in the future is given by $\Delta\widehat{y}_{i(d,c)} = \widehat{\boldsymbol{\beta}}_c(s_i)'\Delta\bar{\mathbf{z}}_{i(d,c)}$, where $\widehat{\boldsymbol{\beta}}_c(s_i)$ measures climate sensitivity of crop yields in observable (historical) period $c$.[16] This predicted log-yield change is converted to the percentage yield change from the present period $c$ to the future period $d$ using $\left(\exp\{\Delta\widehat{y}_{i(d,c)}\} - 1\right) \times 100\%$.

Since the increasing frequency and magnitude of overheat is a key feature of the expected climate change and also a major factor affecting crop yields (Schlenker and Roberts, 2009; Burke and Emerick, 2016), we first examine the impact of future overheat GDD changes on yields. The left panel of Table 5 reports projections

[16] We recover $\widehat{\boldsymbol{\beta}}_c(s_i)$ using functional parameters in (5) as $\widehat{\boldsymbol{\beta}}_c(s_i) = \widehat{\boldsymbol{\beta}}_a(s_i) + \widehat{\boldsymbol{\beta}}^*_{(c,a)}(s_i)$.

Table 5. Projections of the Impact of Future Rising Overheat Temperature on Crop Yields

| | *Spatiotemporally Varying* Model $S_1T_1$ | | | | *Spatially Invariant* Model $S_0T_1$ |
|---|---|---|---|---|---|
| | Weighted Mean | 1st Qu. | Median | 3rd Qu. | Weighted Mean |
| | | | **Corn** | | |
| Had RCP 4.5 | –8.65 (–19.32, 15.75) | –39.27 (–48.95, –18.59) | –22.22 (–39.05, 0.29) | 1.94 (–19.89, 19.40) | –41.88 (–60.97, –17.03) |
| Had RCP 8.5 | –11.39 (–25.24, 22.41) | –49.81 (–61.13, –22.94) | –27.79 (–47.05, –2.19) | 2.32 (–24.97, 25.01) | –51.41 (–71.39, –21.98) |
| Nor RCP 4.5 | –4.77 (–8.54, 2.96) | –16.58 (–20.8, –7.43) | –8.42 (–15.98, 0.17) | 0.65 (–6.14, 5.88) | –17.45 (–28.28, –6.38) |
| Nor RCP 8.5 | –11.07 (–17.98, 6.15) | –30.30 (–38.67, –12.6) | –15.79 (–29.33, 0.28) | 1.30 (–12.89, 12.88) | –36.75 (–54.81, –14.58) |
| | | | **Soybeans** | | |
| Had RCP 4.5 | –47.13 (–63.72, –30.21) | –55.86 (–69.75, –37.08) | –49.41 (–64.39, –29.95) | –40.77 (–57.89, –20.30) | –41.84 (–59.44, –14.73) |
| Had RCP 8.5 | –57.87 (–74.35, –38.21) | –68.68 (–82.82, –48.46) | –60.68 (–75.52, –38.23) | –51.08 (–68.4, –29.14) | –53.49 (–72.04, –20.15) |
| Nor RCP 4.5 | –17.24 (–25.2, –8.03) | –20.83 (–28.24, –9.85) | –17.7 (–25.92, –8.41) | –14.9 (–23.17, –8.44) | –17.4 (–27.26, –5.46) |
| Nor RCP 8.5 | –38.55 (–53.27, –20.27) | –46.39 (–58.7, –25.96) | –39.79 (–53.74, –21.45) | –31.89 (–48.41, –17.19) | –37.53 (–54.31, –12.91) |
| | | | **Cotton** | | |
| Had RCP 4.5 | –22.25 (–58.48, 6.96) | –55.17 (–69.14, –45.88) | –25.89 (–58.5, 8.49) | 25.23 (–50.02, 134.63) | 46.54 (–41.07, 270.9) |
| Had RCP 8.5 | –27.02 (–70.72, 17.58) | –63.27 (–83.74, –50.39) | –38.18 (–75.95, 9.03) | 41.54 (–62.96, 272.68) | 67.65 (–51.09, 488.51) |
| Nor RCP 4.5 | –10.87 (–28.99, –0.46) | –30.20 (–41.33, –23.22) | –9.39 (–25.8, 3.63) | 6.74 (–20.08, 29.05) | 15.94 (–18.51, 66.10) |
| Nor RCP 8.5 | –12.33 (–44.61, 8.94) | –37.68 (–52.24, –29.88) | –16.79 (–41.83, 5.66) | 16.60 (–36.18, 80.32) | 27.09 (–28.23, 127.56) |

*Notes*: The left panel summarizes point estimates of the projected change (in %) in crop yields due to changes in overheat GDD (i.e., $\mathrm{GDD}_{r_0\,°\mathrm{C}+}$) based on the spatiotemporally varying model $S_1T_1$, using the predicted future weather data from two global climate models, HadGEM2-ES365 and NorESM1-M, under two warming scenarios: RCP4.5 (mild warming) and RCP8.5 (severe warming). The right panel reports the counterpart estimates based on the spatially invariant but time-varying model $S_0T_1$. Projections of the change in yields from the present period $c$ (2015–2019) to the future period $d$ (2048–2052) are computed as $\left(\exp\{\Delta\widehat{y}_{i(d,c)}|_{\mathrm{GDD}_{r_0\,°\mathrm{C}+}}\} - 1\right) \times 100\%$, where $\Delta\widehat{y}_{i(d,c)}|_{\mathrm{GDD}_{r_0\,°\mathrm{C}+}} = \left(\widehat{\beta}_c(s_i) \text{for } \mathrm{GDD}_{r_0\,°\mathrm{C}+}\right) \times \Delta(\overline{\mathrm{GDD}_{r_0\,°\mathrm{C}+}})_{i(d,c)}$. Weighted mean is calculated using crop acreages in 2017. Two-sided 95% bias-corrected confidence intervals clustered at the climate division level are in parentheses.

based on the $S_1T_1$ model which flexibly accounts for spatial heterogeneity, while the right panel reports counterpart projections based on its spatially invariant alternative $S_0T_1$. Aside from the obvious finding that projected effect sizes are generally larger under a more severe warming scenario, we can make a few other notable observations here. First, our projections of future yield changes due to global warming are not always statistically different from zero, even under severe scenarios. This is especially the case for production of corn and cotton. Second, the most negative and significant impacts on yields in the future are predicted for soybeans. In contrast, in many cotton-producing counties, we actually project yield *gains*, albeit not all such county-level projections are statistically significant. Third, comparing the results across the two models, we see that the weighted mean projections from the $S_1T_1$ model are generally smaller in magnitude than those produced by the $S_0T_1$ specification à la Yu et al. (2021). This suggests that conventional space-invariant approaches, which confine local heterogeneity strictly to intercept-shifting fixed effects under the assumption that any potential slope heterogeneity is orthogonal to climate (see the discussion in Section 2), may be overestimating future damages of rising overheat temperatures.

We visualize the results in Table 5 in Figure 6 that maps local projections from our $S_1T_1$ model for each crop, with statistically insignificant predictions—regardless of their sign or magnitude—colored using the same shade of gray. Unsurprisingly, the figure reveals that the yield impact of future overheat changes is not spatially homogeneous. In the case of corn production, regions in the lower Midwest (Nebraska, Kansas, southern Iowa, northern Missouri and parts of South Dakota) and the South (Tennessee, Georgia, South Carolina, northern Alabama) are projected to experience large declines in yields by 2050. Whereas, parts of the Corn Belt including some areas in Indiana, Ohio, Illinois, as well as parts of North Dakota are, in contrast, expected to benefit from significant gains in crop yields. Given this spatial bifurcation in future climate change effects on corn productivity with the offset potential in the net, it is unsurprising that we find statistically insignificant (effectively zero) projections *on average* (see the first column in Table 5). There is evidence of similarly bifurcated effects on cotton yields too, with Georgia and North Carolina predicted to experience yield losses, while the producers in more western regions (Arkansas, Oklahoma, and Texas) are to see their cotton yields increase due to changes in overheat GDD. Consistent with Table 5, when statistically different from zero, local county-level projections for soybean yields are mostly negative, which is why the average projection for the U.S. is also significantly negative. The largest decline is to occur in the area of Illinois, Indiana, Ohio as well as Kansas. Minnesota is essentially the only state for which we project a mild yield increase in soybean production. The geographical pattern in the yield impact seen in Figure 6 is largely consistent with that for historical overheat adaptation seen in first-row maps in Figure 4. That is, areas with the largest projected future yield decreases strongly overlaps with areas that historically experienced small or statistically insignificant adaptation to overheat.

Total projections of future yield changes inclusive of the effects of normal temperatures and precipitation (in addition to overheat) are, expectedly, quite similar to projections using only overheat GDD change (see Table G.3 and Figure G.2 in Appendix G), corroborating earlier studies such as Schlenker and Roberts (2009) and Burke and Emerick (2016) documenting that overheat is the major factor influencing crop yields

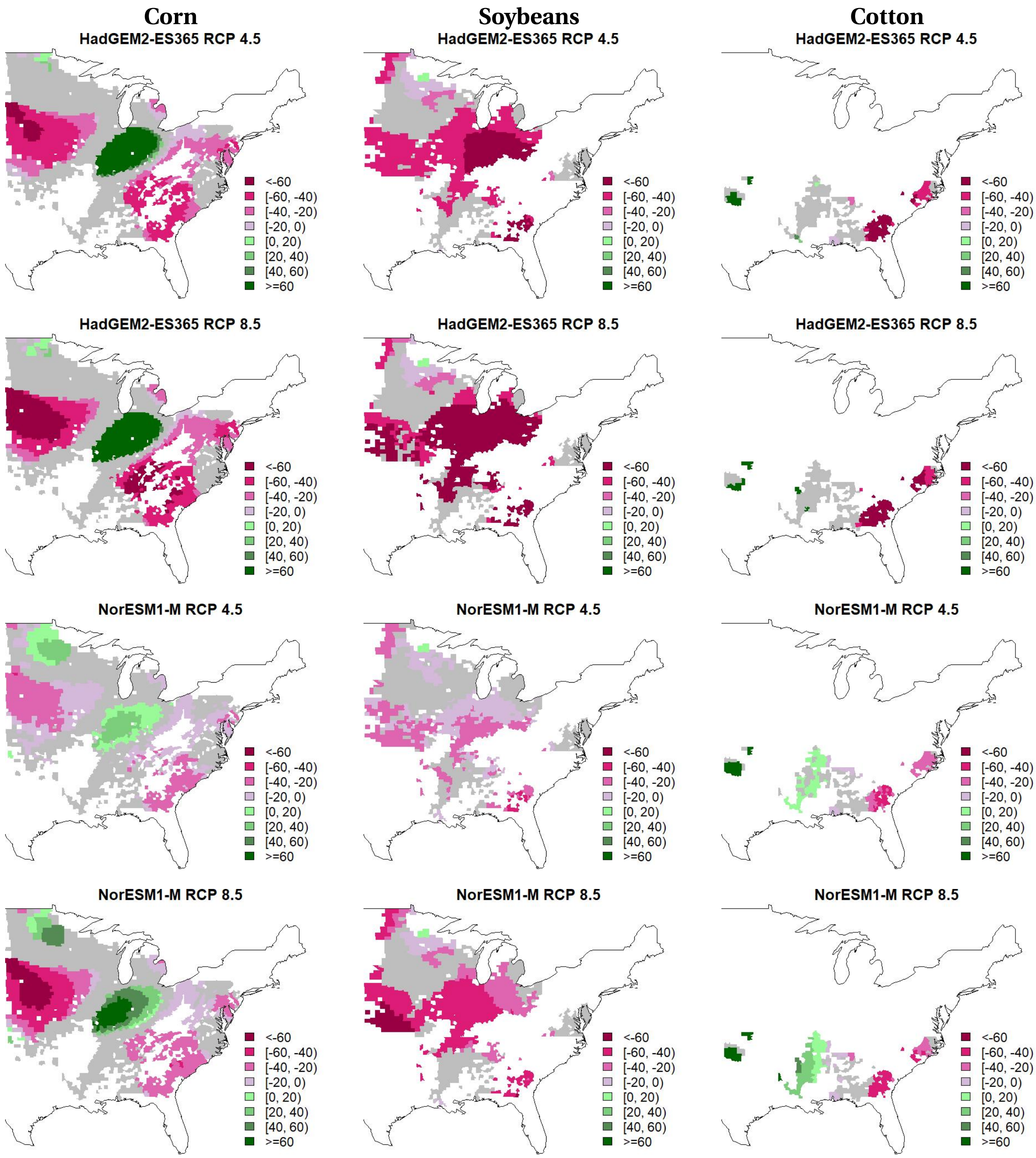


Figure 6. Spatial Distributions of Projections of the Future Rising Overheat Temperature Impact on Crop Yields

*Notes:* Maps plot point estimates of the projected change (in %) in crop yields due to changes in overheat GDD (i.e., $\mathrm{GDD}_{r_0{}^\circ\mathrm{C}+}$) based on the spatiotemporally varying model $S_1T_1$, using the predicted future weather data from two global climate models, HadGEM2-ES365 and NorESM1-M, under two warming scenarios: RCP4.5 (mild warming) and RCP8.5 (severe warming). Projections of the change in yields from the present period $c$ (2015–2019) to the future period $d$ (2048–2052) are computed as $\left(\exp\{\Delta\widehat{y}_{i(d,c)}|_{\mathrm{GDD}_{r_0{}^\circ\mathrm{C}+}}\} - 1\right) \times 100\%$, where $\Delta\widehat{y}_{i(d,c)}|_{\mathrm{GDD}_{r_0{}^\circ\mathrm{C}+}} = \left(\widehat{\beta}_c(s_i)\text{for } \mathrm{GDD}_{r_0{}^\circ\mathrm{C}+}\right) \times \Delta(\overline{\mathrm{GDD}_{r_0{}^\circ\mathrm{C}+}})_{i(d,c)}$. Regardless of their magnitude or sign, all statistically insignificant projections (at the 5% level) are shown using the same shade of gray.

Table 6. Total Projections of the Future Climate Change Impact on Crop Yields

| | Model | **Corn** | **Soybeans** | **Cotton** |
|---|---|---|---|---|
| Had RCP 4.5 | $S_1T_1$ (preferred model) | –11.47 | –38.13 | 19.06 |
| | | (–24.09, 12.61) | (–55.80, –19.85) | (–23.59, 57.89) |
| | $S_0T_1$ (à la Yu et al. (2021)) | –32.08 | –36.18 | 77.24 |
| | | (–49.64, –8.46) | (–55.26, –12.34) | (–11.27, 269.71) |
| | $S_0T_0$ (à la Burke and Emerick's (2016)) | –88.29 | –88.67 | –14.75 |
| | | (–94.35, –74.52) | (–95.06, –73.08) | (–76.73, 434.1) |
| Had RCP 8.5 | $S_1T_1$ (preferred model) | –12.64 | –47.85 | 16.45 |
| | | (–27.50, 16.68) | (–66.50, –25.68) | (–42.45, 77.69) |
| | $S_0T_1$ (à la Yu et al. (2021)) | –40.98 | –47.26 | 107.97 |
| | | (–60.67, –11.88) | (–68.43, –17.01) | (–25.85, 483.21) |
| | $S_0T_0$ (à la Burke and Emerick's (2016)) | –95.13 | –96.17 | –54.70 |
| | | (–98.13, –85.99) | (–98.82, –86.88) | (–91.94, 613.94) |
| Nor RCP 4.5 | $S_1T_1$ (preferred model) | –7.29 | –11.75 | 4.66 |
| | | (–12.95, 1.47) | (–19.63, –3.50) | (–10.98, 13.96) |
| | $S_0T_1$ (à la Yu et al. (2021)) | –11.04 | –13.57 | 25.29 |
| | | (–19.78, –1.11) | (–24.40, –3.45) | (–3.30, 62.93) |
| | $S_0T_0$ (à la Burke and Emerick's (2016)) | –28.29 | –37.62 | –4.44 |
| | | (–44.97, –5.62) | (–53.67, –17.51) | (–39.24, 83.28) |
| Nor RCP 8.5 | $S_1T_1$ (preferred model) | –11.61 | –28.58 | 23.88 |
| | | (–20.50, 6.37) | (–43.90, –11.35) | (–5.75, 45.61) |
| | $S_0T_1$ (à la Yu et al. (2021)) | –26.09 | –30.52 | 49.02 |
| | | (–42.38, –4.93) | (–49.81, –8.57) | (–3.14, 129.45) |
| | $S_0T_0$ (à la Burke and Emerick's (2016)) | –68.30 | –76.33 | 21.54 |
| | | (–83.12, –38.20) | (–88.68, –50.07) | (–46.56, 374.35) |

*Notes*: The table reports weighted averages (in %) of the projected change in crop yields due to climate change based on models $S_1T_1$, $S_0T_1$ and $S_0T_0$. We use predicted future weather data from two global climate models, HadGEM2-ES365 and NorESM1-M, under two warming scenarios: RCP4.5 (mild warming) and RCP8.5 (severe warming). Projections of the change in yields from the present period $c$ (2015–2019) to the future period $d$ (2048–2052) are computed as $\left(\exp\{\Delta\widehat{y}_{i(d,c)}\}-1\right)\times 100\%$, where $\Delta\widehat{y}_{i(d,c)} = \widehat{\boldsymbol{\beta}}_c(s_i)\Delta\bar{\mathbf{z}}_{i(d,c)}$. Weighted mean is calculated using crop acreages in 2017. Two-sided 95% bias-corrected confidence intervals clustered at the climate division level are in parentheses.

in a warming climate.[17]

To draw conclusions about a "representative" county that would correspond to the object of analysis of conventional spatially invariant methodologies that argue to focus on *average* causal effects of climate, in Table 6 we aggregate local county-specific projections, weighting them using crop acreage in 2017 (the midpoint of the "present" 2015–2019 period). For comparison, we include total projections from our preferred model $S_1T_1$ as well as the $S_0T_1$ and $S_0T_0$ alternatives. Average yield loss projections for corn based on our spatiotemporally varying methodology are smaller than those obtained using these two alternative models.[18] Our model projects total yield losses for corn ranging from –7% to –13% and, notably, these losses are statistically *in*significant even under severe global warming scenarios. As discussed above, this statisti-

[17]Note that Table G.3 in Appendix G shows that the future climate change by 2050 is predicted to result in a statistically significant median decrease in corn yields, although the weighted average decrease is still insignificant.

[18]Overall, a time-invariant $S_0T_0$ model tends to predict much larger yield losses than time-varying $S_0T_1$ and $S_1T_1$ models. This is because, as first documented by Yu et al. (2021) and corroborated by our findings, time-varying models allow for historical adaptation which feeds into the computation of future projections through estimates of the "present" yield-climate relationship.

cally insignificant result is largely due to bifurcated effects of a changing climate on corn yields, with some regions experiencing yield losses and others gains (also see Figures 6 and G.2).

For soybean yields, our $S_1T_1$ model projects the smallest yield losses among three specifications under both HadGEM2-ES365 scenarios. But under NorESM1-M scenarios, it projects slightly larger yield losses than those by $S_0T_1$, although these projections are still less than half of what the time-invariant $S_0T_0$ alternative predicts (see the "Soybeans" column in Table 6). As projected by our model, the future soybean yield reduction expected in a typical county ranges between statistically significant 12% and 48%. For cotton, two time-varying models ($S_0T_1$ and $S_1T_1$) project yield gains while the time-invariant model ($S_0T_0$) generally project yield losses. When comparing projections from time-varying models, we find that a spatially-invariant $S_0T_1$ model tends to overestimate future cotton yield changes, sometimes projecting unrealistically large (over 100%) yield gains. Although, regardless of whether non-neutral spatial heterogeneity is accounted for or not, these weighted average projections are statistically insignificant.

Overall, total projections of future climate change impacts on corn yields from our spatiotemporally varying model are much smaller than those reported in earlier studies. For instance, Yu et al. (2021), employing a $S_0T_1$-like approach, document that climate change would lead to a 39%–68% yield loss for corn and a 86%–92% yield loss for soybeans by 2050 relative to yields in 2013–2017. Burke and Emerick (2016), using a $S_0T_0$-like model, report 7% to 64% of corn yield reduction by 2050. Although our projections are not perfectly comparable to these studies due to differences in data and future climate change scenarios used in analyses, most of these differences are likely attributable to our reliance on more granular measurements of local heat sensitivity of crop yields and their adaptation thereto when projecting future losses, instead of using globally "average" coefficients. Because areas with high acreage and high yield tend to adapt more as shown in our results, a weighted aggregate of local yield loss projections that accounts for this spatial heterogeneity provides an expectedly smaller—an arguably, more accurate—average projection. This finding of significantly smaller yield damages underscores the importance of considering non-neutral spatial heterogeneity in studying the yield-climate relationship.

## 6 Concluding Remarks

Although many prior studies have examined whether, or to what extent, adaptation to climate change occurs, most exclusively focus on identification of the *average* adaptation, pooling over farmers located across different geographic locations. Such a global estimand sheds little light on local adaptation experiences of farmers that exhibit substantial heterogeneity. Understanding this (naturally occurring) spatial heterogeneity is important for producing more granular measurements of historical adaptation and, by extension, more accurate projections of expected yield losses associated with a warming climate, particularly in large and climatically diverse countries. This paper extends the literature by providing novel evidence of explicitly spatial heterogeneity in heat sensitivity of U.S. agriculture and its adaptation to climate change. We accomplish this by generalizing a popular long-differences methodology to explicitly incorporate geographic information of crop-producing counties in a flexible semiparametric fashion, which we implement using local kernel averaging. This lets us control for spatially clustered, local heterogeneity that may be non-neutral.

Based on data for the rain-fed region of the United States in 1958–2019, we show significant cross-location heterogeneity in climate sensitivity of crop yields and their adaptation to climate change. For corn, soybeans, and cotton, 54%, 75%, and only 23% of producing counties, respectively, are estimated to have experienced a statistically significant decrease in overheat sensitivity of yields, thereby adapting to a warming climate. The remaining counties experienced either statistically significant increases (i.e., maladaptation) or no changes in overheat sensitivity (i.e., no adaptation). Geographically, corn and soybean adaptation mainly occurred in the Northern Great Plains and Upper Midwest; for cotton, it mainly occurred in Arkansas, Louisiana, and Mississippi. On acreage-weighted average, our model estimates that overheat sensitivity of corn, soybeans, and cotton yields decreased by 73%, 49%, and 51%, respectively, although for cotton the decrease is statistically insignificant.

Importantly, we find that measurements of (mal)adaptation produced by traditional spatially invariant specifications tend to be larger, suggesting the potential to overestimate (mal)adaptation when abstracting away from naturally occurring non-neutral spatial heterogeneity. Relatedly, in most cases, projections of future climate change impacts on crop yields by 2050 based on our spatially flexible model are the smallest compared to popular alternative specifications, and are statistically insignificant for corn and cotton. This suggests that existing projections of yield loss due to climate change, and thereby the expected social cost of carbon, are likely overestimated. For example, Rennert et al. (2022) estimate the social cost of carbon to be $185 per ton of $CO_2$, among which $84 (about 45%) is attributed to an agricultural impact of climate change. Our findings could therefore have important implications for reassessing social costs of carbon.

## 7 Acknowledgments

We thank Ellen Bruno, Marshall Burke, Walter Falcon, Brittney Goodrich, Nic Irwin, David Lobell, Bruce McCarl, Rodolfo Nayga, Sofia Villas-Boas, and Brian Wright for constructive comments. We are grateful to Wendiam Sawadgo for his support with the cover crop data and to Yong Liu for his help with the GE crop adoption data. We also thank seminar participants at Stanford University, Texas A&M University, UC Berkeley, UC Davis, University of Wisconsin-Madison, the 2022 AAEA Annual Meeting, the AERE 2022 Summer Conference, and the 2023 NC1034 Annual Meeting and Research Conference for helpful feedback.

**Disclosure Statement.** The authors report there are no competing interests to declare.

## References

Aldana, U., Foltz, J. D., Barham, B. L., and Useche, P. (2011). Sequential adoption of package technologies: The dynamics of stacked trait corn adoption. *American Journal of Agricultural Economics*, 93(1):130–143.

Annan, F. and Schlenker, W. (2015). Federal crop insurance and the disincentive to adapt to extreme heat. *American Economic Review*, 105(5):262–66.

Blanc, E. and Schlenker, W. (2017). The use of panel models in assessments of climate impacts on agriculture. *Review of Environmental Economics and Policy*, 11(2):258–279.

Blanco-Canqui, H., Shaver, T. M., Lindquist, J. L., Shapiro, C. A., Elmore, R. W., Francis, C. A., and Hergert, G. W. (2015). Cover crops and ecosystem services: Insights from studies in temperate soils. *Agronomy Journal*, 107(6):2449–2474.

Bogdanski, A. (2012). Integrated food–energy systems for climate-smart agriculture. *Agriculture & Food Security*, 1(1):1–10.

Burke, M. and Emerick, K. (2016). Adaptation to climate change: Evidence from US agriculture. *American Economic Journal: Economic Policy*, 8(3):106–40.

Butler, E. E. and Huybers, P. (2013). Adaptation of US maize to temperature variations. *Nature Climate Change*, 3(1):68–72.

Cai, Z., Fan, J., and Li, R. (2000). Efficient estimation and inferences for varying-coefficient models. *Journal of the American Statistical Association*, 95(451):888–902.

Chemeris, A., Liu, Y., and Ker, A. P. (2022). Insurance subsidies, climate change, and innovation: Implications for crop yield resiliency. *Food Policy*, 108:102232.

Chen, S., Chen, X., and Xu, J. (2016). Impacts of climate change on agriculture: evidence from China. *Journal of Environmental Economics and Management*, 76:105–124.

Chen, S. and Gong, B. (2021). Response and adaptation of agriculture to climate change: Evidence from China. *Journal of Development Economics*, 148:102557.

Cherr, C., Scholberg, J. S., and McSorley, R. (2006). Green manure approaches to crop production: A synthesis. *Agronomy Journal*, 98(2):302–319.

Connor, L. and Katchova, A. L. (2020). Crop insurance participation rates and asymmetric effects on US corn and soybean yield risk. *Journal of Agricultural and Resource Economics*, 45(1):1–19.

Cui, X. (2020). Climate change and adaptation in agriculture: Evidence from US cropping patterns. *Journal of Environmental Economics and Management*, 101:1–24.

Cui, X. and Xie, W. (2022). Adapting agriculture to climate change through growing season adjustments: Evidence from corn in China. *American Journal of Agricultural Economics*, 104(1):249–272.

Dabney, S. M., Delgado, J. A., and Reeves, D. W. (2001). Using winter cover crops to improve soil and water quality. *Communications in Soil Science and Plant Analysis*, 32(7-8):1221–1250.

Decker, H. L., Gamble, A. V., Balkcom, K. S., Johnson, A. M., and Hull, N. R. (2022). Cover crop monocultures and mixtures affect soil health indicators and crop yield in the southeast united states. *Soil Science Society of America Journal*, 86(5):1312–1326.

Economic Research Service (2022). Cotton sector at a glance. Online document of the U.S. Department of Agriculture, available at: https://www.ers.usda.gov/topics/crops/cotton-wool/cotton-sector-at-a-glance/ (accessed October 8, 2022).

Efron, B. (1982). *The jackknife, the bootstrap and other resampling plans.* The Society for Industrial and Applied Mathematics (SIAM), Philadelphia, PA.

Field, C. B., Barros, V., Stocker, T. F., and Dahe, Q. (2012). *Managing the risks of extreme events and disasters to advance climate change adaptation: Special report of the intergovernmental panel on climate change.* Cambridge University Press.

Ghosh, P. N., Miao, R., and Malikov, E. (2023). Crop insurance premium subsidy and irrigation water withdrawals in the western united states. *The Geneva Papers on Risk and Insurance–Issues and Practice*, 48:968–992.

Goodwin, B. K. and Piggott, N. E. (2020). Has technology increased agricultural yield risk? Evidence from the crop insurance Biotech Endorsement. *American Journal of Agricultural Economics*, 102(5):1578–1597.

Goodwin, B. K., Vandeveer, M. L., and Deal, J. L. (2004). An empirical analysis of acreage effects of participation in the federal crop insurance program. *American Journal of Agricultural Economics*, 86(4):1058–1077.

Gourdji, S. M., Sibley, A. M., and Lobell, D. B. (2013). Global crop exposure to critical high temperatures in the reproductive period: historical trends and future projections. *Environmental Research Letters*, 8(2):024041.

Hall, P., Li, Q., and Racine, J. S. (2007). Nonparametric estimation of regression functions in the presence of irrelevant regressors. *The Review of Economics and Statistics*, 89(4):784–789.

Hastie, T. and Tibshirani, R. (1993). Varying-coefficient models. *Journal of the Royal Statistical Society. Series B (Methodological)*, 55(4):757–796.

Jian, J., Lester, B. J., Du, X., Reiter, M. S., and Stewart, R. D. (2020). A calculator to quantify cover crop effects on soil health and productivity. *Soil and Tillage Research*, 199:104575.

Keane, M. and Neal, T. (2020). Climate change and US agriculture: Accounting for multidimensional slope heterogeneity in panel data. *Quantitative Economics*, 11(4):1391–1429.

Lee, S., Ji, Y., and Moschini, G. (2022). Agricultural innovation and adaptation to climate change: Insights from us maize. *Journal of the Agricultural and Applied Economics Association*, 1(2):165–179.

Li, Q., Huang, C. J., Li, D., and Fu, T.-T. (2002). Semiparametric smooth coefficient models. *Journal of*

*Business & Economic Statistics*, 20(3):412–422.

Li, Q. and Racine, J. S. (2007). *Nonparametric Econometrics: Theory and Practice*. Princeton University Press, Princeton.

Li, Q. and Racine, J. S. (2010). Smooth varying-coefficient estimation and inference for qualitative and quantitative data. *Econometric Theory*, 26:1607–1637.

Lobell, D. B., Deines, J. M., and Tommaso, S. D. (2020). Changes in the drought sensitivity of US maize yields. *Nature Food*, 1(11):729–735.

Lobell, D. B., Roberts, M. J., Schlenker, W., Braun, N., Little, B. B., Rejesus, R. M., and Hammer, G. L. (2014). Greater sensitivity to drought accompanies maize yield increase in the u.s. midwest. *Science*, 344(6183):516–519.

Malikov, E., Kumbhakar, S. C., and Sun, Y. (2016). Varying coefficient panel data model in the presence of endogenous selectivity and fixed effects. *Journal of Econometrics*, 190:233–251.

Malikov, E., Miao, R., and Zhang, J. (2020). Distributional and temporal heterogeneity in the climate change effects on US agriculture. *Journal of Environmental Economics and Management*, 104:102386.

Mammen, E. (1993). Bootstrap and wild bootstrap for high dimensional linear models. *The Annals of Statistics*, 21(1):255–285.

Martin, J. H. and Leonard, W. H. (1949). *Principles of field crop production*. Macmillan, New York.

Martinez-Feria, R. A., Dietzel, R., Liebman, M., Helmers, M. J., and Archontoulis, S. V. (2016). Rye cover crop effects on maize: A system-level analysis. *Field Crops Research*, 196:145–159.

Mendelsohn, R., Nordhaus, D., and Shaw, D. (1994). The impact of global warming on agriculture: A ricardian analysis. *American Economic Review*, 84(4):753–771.

Mérel, P. and Gammans, M. (2021). Climate econometrics: Can the panel approach account for long-run adaptation? *American Journal of Agricultural Economics*, 103(4):1207–1238.

Miao, R. (2020). Climate, insurance and innovation: The case of drought and innovations in drought-tolerant traits in US agriculture. *European Review of Agricultural Economics*, 47(5):1826–1860.

Miao, R., Khanna, M., and Huang, H. (2016). Responsiveness of crop yield and acreage to prices and climate. *American Journal of Agricultural Economics*, 98(1):191–211.

Moscona, J. and Sastry, K. (2022). Does directed innovation mitigate climate damage? Evidence from US agriculture. *Quarterly Journal of Economics*, forthcoming.

Natural Resources Conservation Service (2018). National soil survey handbook. *U.S. Department of Agriculture*.

Park, Y., Li, B., and Li, Y. (2023). Crop yield prediction using bayesian spatially varying coefficient models with functional predictors. *Journal of the American Statistical Association*, 118:70–83.

Rahmstorf, S. and Coumou, D. (2011). Increase of extreme events in a warming world. *Proceedings of the National Academy of Sciences*, 108(44):17905–17909.

Reeves, D. (2018). Cover crops and rotations. *Crops Residue Management*, pages 125–172.

Rennert, K., Errickson, F., Prest, B. C., Rennels, L., Newell, R. G., Pizer, W., Kingdon, C., Wingenroth, J., Cooke, R., Parthum, B., Smith, D., Cromar, K., Diaz, D., Moore, F. C., Müller, U. K., Plevin, R. J., Raftery, A. E., Ševčíková, H., Sheets, H., Stock, J. H., Tan, T., Watson, M., Wong, T. E., and Anthoff, D. (2022). Comprehensive evidence implies a higher social cost of co2. *Nature*, 610(7933):687–692.

Roberts, M. J. and Schlenker, W. (2011). The evolution of heat tolerance of corn: Implications for climate change. In Libecap, G. D. and Steckel, R. H., editors, *The Economics of Climate Change: Adaptations Past and Present*, pages 225–251. University of Chicago Press, Chicago, IL.

Roberts, M. J. and Schlenker, W. (2012). Is agricultual production becoming more or less sensitive to extreme heat? evidence from u.s. corn and soybean yields. In Fullerton, D. and Wolfram, C., editors, *The Design and Implementation of U.S. Climate Policy*, pages 271–282. University of Chicago Press, Chicago, IL.

Rodríguez-Póo, J. M. and Soberón, A. (2015). Nonparametric estimation of fixed effects panel data varying coefficient models. *Journal of Multivariate Analysis*, 133:95–122.

Scherr, S. J., Shames, S., and Friedman, R. (2012). From climate-smart agriculture to climate-smart landscapes. *Agriculture & Food Security*, 1(1):1–15.

Schlenker, W. and Roberts, M. J. (2009). Nonlinear temperature effects indicate severe damages to US crop yields under climate change. *Proceedings of the National Academy of Sciences*, 106(37):15594–15598.

Seifert, C. A., Azzari, G., and Lobell, D. B. (2018). Satellite detection of cover crops and their effects on crop yield in the midwestern united states. *Environmental Research Letters*, 13(6):1–9.

Semenov, M. A. and Shewry, P. R. (2011). Modelling predicts that heat stress, not drought, will increase vulnerability of wheat in Europe. *Scientific Reports*, 1(1):1–5.

Su, L. and Ullah, A. (2011). Nonparametric and semiparametric panel econometric models: Estimation and testing. In Ullah, A. and Giles, D. E. A., editors, *Handbook of Empirical Economics and Finance*, pages 455–497. Taylor and Francis Group, New York.

Sun, Y., Carroll, R. J., and Li, D. (2009). Semiparametric estimation of fixed-effects panel data varying coefficient models. *Advances in Econometrics*, 25:101–129.

Trnka, M., Rötter, R. P., Ruiz-Ramos, M., Kersebaum, K. C., Olesen, J. E., Žalud, Z., and Semenov, M. A. (2014). Adverse weather conditions for European wheat production will become more frequent with climate change. *Nature Climate Change*, 4(7):637–643.

Ullah, A. (1985). Specification analysis of econometric models. *Journal of Quantitative Economics*, 1(2):187–209.

Unger, P. W. and Vigil, M. F. (1998). Cover crop effects on soil water relationships. *Journal of Soil and Water Conservation*, 53(3):200–207.

Wagner, G. and Schlenker, W. (2022). Declining crop yields limit bioenergy potential. *Nature*, 609:250–251.

Wallander, S., Smith, D., Bowman, M., and Claassen, R. (2021). Cover crop trends, programs, and practices in the united states. Economic Information Bulletin Number 222, Economic Research Service, the U.S. Department of Agriculture.

Weber, J. G., Key, N., and O'Donoghue, E. (2016). Does federal crop insurance make environmental externalities from agriculture worse? *Journal of the Association of Environmental and Resource Economists*, 3(3):707–742.

World Bank (2008). Local institutions and climate change adaptation. *Social Development Notes – The Social Dimensions of Climate Change*, 113.

Yu, C., Miao, R., and Khanna, M. (2021). Maladaptation of US corn and soybeans to a changing climate. *Scientific Reports*, 11(1):1–12.